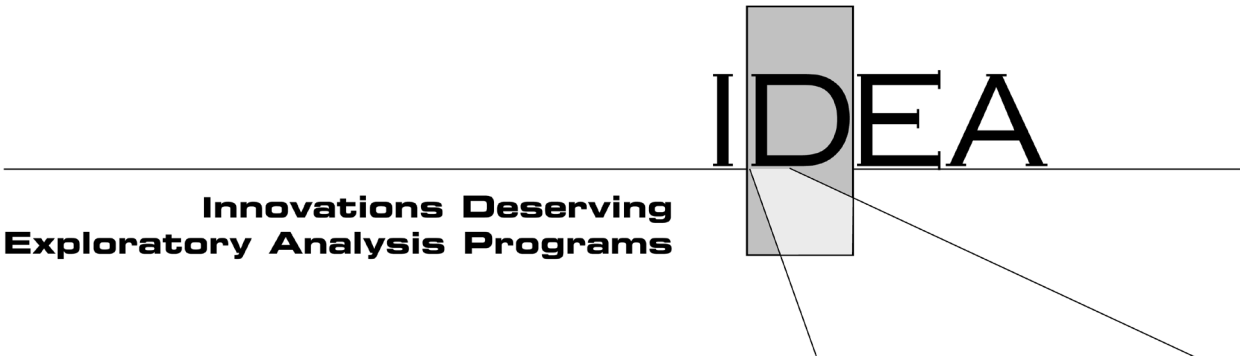

Transit IDEA Program

SAFETY ASSESSMENT OF THE INTERACTION BETWEEN THE AUTONOMOUS SHUTTLE BUS AND VULNERABLE ROAD USERS

Final Report for
Transit IDEA Project 98

Prepared by:
Sungmoon Jung,
MohammadReza Seyedi, Md.
Mobasshir Rashid
FAMU-FSU College of Engineering

July 2022

NATIONAL ACADEMIES Sciences Engineering Medicine

TRB TRANSPORTATION RESEARCH BOARD

Innovations Deserving Exploratory Analysis (IDEA) Programs Managed by the Transportation Research Board

This IDEA project was funded by the Transit IDEA Program.

The TRB currently manages the following three IDEA programs:

- The NCHRP IDEA Program, which focuses on advances in the design, construction, and maintenance of highway systems, is funded by American Association of State Highway and Transportation Officials (AASHTO) as part of the National Cooperative Highway Research Program (NCHRP).
- The Rail Safety IDEA Program currently focuses on innovative approaches for improving railroad safety or performance. The program is currently funded by the Federal Railroad Administration (FRA). The program was previously jointly funded by the Federal Motor Carrier Safety Administration (FMCSA) and the FRA.
- The Transit IDEA Program, which supports development and testing of innovative concepts and methods for advancing transit practice, is funded by the Federal Transit Administration (FTA) as part of the Transit Cooperative Research Program (TCRP).

Management of the three IDEA programs is coordinated to promote the development and testing of innovative concepts, methods, and technologies.

For information on the IDEA programs, check the IDEA website (www.trb.org/idea). For questions, contact the IDEA programs office by telephone at (202) 334-3310.

IDEA Programs
Transportation Research Board
500 Fifth Street, NW
Washington, DC 20001

SAFETY ASSESSMENT OF THE INTERACTION BETWEEN THE AUTONOMOUS SHUTTLE BUS AND VULNERABLE ROAD USERS

TRANSIT IDEA PROGRAM

Final Report

Transit IDEA Project T-98

Prepared for

IDEA Program

TRANSPORTATION RESEARCH BOARD

NATIONAL ACADEMY OF SCIENCES, ENGINEERING, AND MEDICINE

Sungmoon Jung, MohammadReza Seyedi, Md. Mobasshir Rashid

Department of Civil and Environmental Engineering

FAMU-FSU College of Engineering

July 2022

GLOSSARY

AV	*Autonomous Vehicles*
ADS	*Automated Driving Systems*
ASB	*Autonomous Shuttle Bus*
FMVSS	*Federal Motor Vehicle Safety Standards*
FTA	*Federal Transit Administration*
LIDAR	*Light Detection And Ranging*
LSAV	*Low-Speed Automated Vehicle*
JTA	*Jacksonville Transportation Authority*
NHTSA	*National Highway Transportation Safety Administration*
PET	*Post Encroachment Time*
RADAR	*Radio Detection And Ranging*
SAE	*Society of Automotive Engineering*
TTC	*Time to Collision*
VRUs	*Vulnerable Road Users*
SFM	*Social Force Model*
FE	*Finite Element*
HIC	*Head Injury Criteria*
IARV	*Injury Assessment Reference Values*
AIS	*Abbreviated Injury Scale*

PROJECT PERSONNEL

Proposer:	***FAMU-FSU College of Engineering***
Academic Researchers:	***Sungmoon Jung***, *PI,* sjung@eng.famu.fsu.edu *Professor, Department of Civil and Environmental Engineering* ***MohammadReza Seyedi***, *Co-PI,* reza.seyedi@fsu.edu *Postdoc, Department of Civil and Environmental Engineering* ***Md. Mobasshir Rashid***, *Researcher,* mrashid@fsu.edu *Graduate Student, Department of Civil and Environmental Engineering*
Industry Collaborator:	***Jacksonville Transportation Authority***
Industry Team:	***William Frazer***, wfrazer@jtafla.com *Director of Automation* ***Michael Feldman.*** msfeldman@jtafla.com *AVP of Automation*
Expert Panel:	***Santosh Mishra,*** santosh.mishra@ibigroup.com *Associate Director/Practice Lead for Mobility Technologies, IBI Group* ***Louis Sanders,*** lou@aE.Solutions *Director, Business Development, Ayers Electronic Systems,* ***Raj Ponnaluri***, Raj.Ponnaluri@dot.state.fl.us *Connected Vehicles and Arterial Management Engineer,* *Florida Department of Transportation* ***Chris Geraci***, cgeraci@jtafla.com *Chief Safety Officer, Jacksonville Transportation Authority*

PROJECT SUMMARY

Project Objectives

The objective of the project is to assess the safety of autonomous shuttle buses against vulnerable road users (pedestrians/bicyclists). High-risk situations are analyzed to provide recommendations to improve safety.

Project Tasks

Nine tasks have been defined for this project. Based on the IDEA program instruction, these tasks are divided into two stages. The first stage will take about 1 year and the second stage will take 9 months. Details of each task are explained as follows:

Stage 1: Development of the Computer Models and Design the Simulation Plans

Task 1. *Kick-off meeting*

Task 2. *Develop the PC-Crash Models (5 months):* The comprehensive literature review will be conducted to find the current body of knowledge regarding ASB's safety and the 3D kinematic models of the ASB and VRUs. The details of the vehicle, infrastructure, and VRUs parameters will be investigated their computer models will be developed using PC-Crash software.

Task 3. *Design of Simulation Plan (5 months):* The details of the autonomous active safety system including emergency brake algorithm and trajectory systems will be modeled to identify the high risk/ conflicting situations. Our industrial partner's input will be considered to define scenarios and the required field data will be acquired to validate the simulation models and define the simulation process.

Task 4. *Evaluate Transit Properties (3 months):* At this stage, the operational design domain of ASB will be evaluated considering multiple aspects such as:

- Operational condition (considering the risk assessment for different weather conditions)
- Route selection (whether it is a fixed-route or flexible service between two or more points)
- Road specification (Speed limit, communication methods between road users and ASB, etc.)
- Traffic condition
- Passenger/road user perspective

We will incorporate industrial partner's inputs to identify the wide range of parameters that can affect the safe operation bus and will document them to help transit agencies to make informed deployment decisions.

Task 5. Stage I Report: A Stage I draft report will be prepared and submitted by the investigator to the expert review panel for review and comment. Following this review, a revised Stage I final report will be submitted to the Transit IDEA Program, along with expert review panel comments and point-by-point investigator responses. The Stage I report will detail the results and findings of this stage and identify strategies to address any project issues in Stage II.

Stage 2: Risk Assessment, Data Processing, and Safety Recommendations

Task 6. *Collect the Simulation Results and Analyze the Data (6 months):* Conduct series of simulations of ASB-VRU scenarios considering different transit properties, ASB's active safety systems, ASB's speed, and directions, infrastructural factors, and weather conditions. The high-risk scenarios will be identified, and a probabilistic risk assessment will be conducted.

Task 7. *Develop FE Models for Injury Assessment (4 months):* For the cases that unavoidable crashes are more likely to occur, the finite element (FE) model will be developed to quantify the details of injury risks using LS-DYNA software. The FE model and multi-body model of the VRU's will be used to assess the potential injuries that VRUs sustain during those crashes. The results can be used to develop mitigation mechanisms.

Task 8. *Document Findings (2 months):* In this task, the qualitative and quantitative risk assessment will be conducted using simulation data (PC-Crash and Finite Element Analysis) and use-case tests to present a meaningful safety assessment. Effective parameters in reducing the number of high-risk/conflicting situations regarding ASB-VRU interactions will be highlighted and mitigation strategies to reduce the crash risks will be suggested. Finally, although this project is primarily focused on the safety assessment of vulnerable road users, it will produce a document to assist agencies in developing a robust safety evaluation of ASB implementation. The recommendations and research findings resulted from this project can also be used in three different areas:

- Standards regarding the safe operation of ASB
- Supporting infrastructure which involves local DOT and transit agencies
- Regional planning

In addition, we and our industry collaborator will actively reach out to the public and academia (seminar/ webinar/ videos) to increase the public awareness and understanding about the ASB's technologies regarding safe operation. These documents will be prepared to disseminate the findings of the research project to a broad community.

Task 9. *Draft Final Report and Final Report:* The project investigators will prepare and submit a draft final report documenting the results of this project. The draft final report will include the results of all stages of this project, statistical analysis, and potential recommendations. The project investigators will distribute the draft final report to the expert review panel for review and comment. The investigator will address the review comments in a revised draft report and submit the report, along with the point-by-point written responses to review comments, to the Transit IDEA Program Manager no later than 60 days before the completion of the contract. The Transit IDEA Program Manager will distribute the final report to the Transit IDEA Program Oversight Panel for review and comment. The project investigators will provide a point-by-point written response to the review comments and submit a revised Final Report to the Transit IDEA Program Manager. The IDEA programs office will distribute the Draft Final report to the Transit IDEA Program Oversight Panel for balloting. The project investigators will address the Oversight Panel comments in a revised final report and submit the report, along with written responses to review comments, to the IDEA programs office.

TABLE 1: Summary of tasks

Stage 1: *Development of the Computer Models and Design the Simulation Plans*			
Task Number	**Task Item**	**Duration**	
2	Develop the PC-Crash Models (Completed)	5	***12 months***
3	Design of Simulation Plan	5	
4	Evaluate Transit Properties	3	
5	Stage I Report	1	
Stage 2: *Risk Assessment, Data Processing and Safety Recommendations*			
6	Collect the Simulation Results and Analyze the Data	6	***9 months***
7	Develop FE Models for Injury Assessment	4	
8	Document Findings	2	
9	Final Report	1	

Project Schedule

TABLE 2: Project schedule for Transit-98 project

Months	***Timeline***	***Deadlines of***	***Action Items***
	27-Oct-20	Project Started	*Kick-off meeting was held on Nov 6*

3	*27-Jan-21*	Progress Report	*Quarterly report was submitted on Jan*
6	*27-Apr-21*	Progress Report	*Quarterly report was submitted on April*
9	*27-Jul-21*	Progress Report	*Quarterly report was submitted on July*
12	*27-Oct-21*	Stage 1 Report	*Stage 1 report was submitted on October*
15	*27-Jan-22*	Progress Report	*Quarterly report was submitted on January*
17	*27-Mar-22*	Draft Report	*Draft report was submitted on March*
19	*27-May-22*	Draft Final Report	
21	*27-Jul-22*	Final Report	

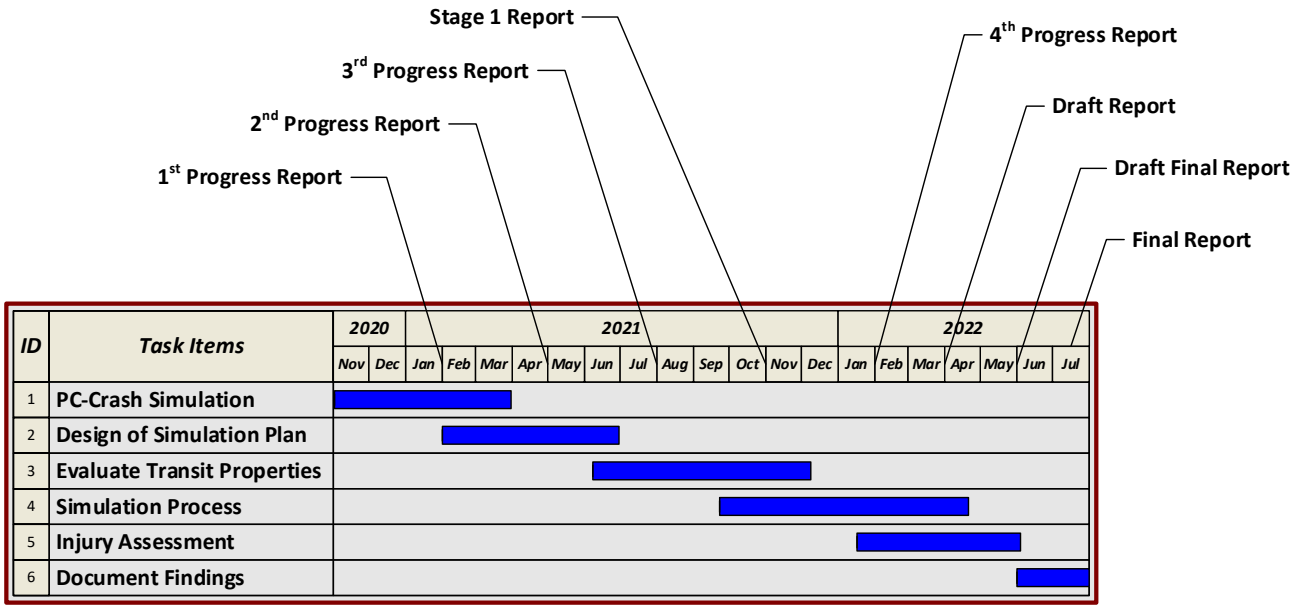

FIGURE 1: Proposed project timeline

TABLE OF CONTENTS

1 EXECUTIVE SUMMARY

In recent years, there has been a growing interest in the deployment of autonomous vehicles (AVs) for public transportation. In the US, transportation agencies are exploring the impacts of incorporating automation on safety or mobility, especially for the low-speed automated vehicles (LSAV) *(1)*. One of the challenges in deploying these vehicles is the safety of vulnerable road users (VRUs). The objectives of this research project were to identify potential safety issues regarding the LSAV-VRUs interactions, and to evaluate the performance of LSAV to provide practical recommendations on improving the safety.

The completed tasks can be divided into three main parts (see FIGURE 2): 1) The close-track tests of autonomous shuttle bus which were conducted by our industry partner JTA. The data were then analyzed qualitatively and quantitively to build our safety risk assessment framework and improve our basic vehicle model; 2) The vehicle and pedestrian models which represent the motion of the vehicle and crossing pedestrian; 3) Field crash data analysis and safety assessment of LSAV to identify the characteristics of relevant transit crashes, transit properties, and extracting contextual information.

One of the challenges of LSAV-VRUs interaction is to validate the safety performance of these vehicles for high-risk scenarios (edge cases). Defining safety tests that could push the capability of LSAV's systems to their limits (while maintaining safety) and understanding their operational design domains (ODD) are the key factors in the safety evaluation process. The goal of most test cases is to validate the basic performance of LSAV's stacks such as perception, planning, and control of the vehicle. Although this is a critical step towards a safe deployment, vehicle-level testing alone would not be enough to ensure safety. The framework proposed in this research (see FIGURE 2) includes the computer simulation, which enables exploration of safety-critical cases. The computer simulation consists of modeling the overall motion and basic decision-making process of the vehicle and pedestrian. Minimum gaps that pedestrians accept during road crossing were obtained from the MATLAB simulation model. A finite element simulation model was developed to determine risk injury criteria for both head and chest if an unavoidable crash was to occur. Using the simulation and field crash data we were able to identify scenarios that can lead to hazardous situations regarding the pedestrians. The crossing, the bus station, and the roundabout were the most challenging type of interactions that LSAV's can have regarding pedestrian interaction. A systematic pedestrian safety analysis such as the analyses conducted in this study can help improve safety of pedestrians. This research analyzed selected cases, but the findings are case-specific and need to be repeated for new cases or different types of vehicles.

The main lessons learned in this research were as follows. First, the driver must have minimum interaction with the vehicle for a fully automated low-speed vehicle. This means that the vehicle must be able to operate safely in most traffic situations without requiring driver assistance. Second, for safe operation of LSAV, sufficient knowledge and data on pedestrians are necessary far beyond what is covered in this research. This may require inter-jurisdictional collaboration amongst state DOTs and other transit agencies. The knowledge and data can be shared to obtain critical information about the safety performance of different LSAV types in different edge case scenarios and understand the important key aspects of their ODD. Third, how road users feel safe when interacting with LSAV has a subjective nature. For example, how far away an LSAV should stop when a pedestrian is crossing in front of the vehicle highly

depends on how closeness can affect the perception of comfort and safety for that specific road user. This is a challenging aspect that the developers of these technologies must address. While road users may not experience actual accidents, they can form negative opinions on the LSAV if they do not feel safe.

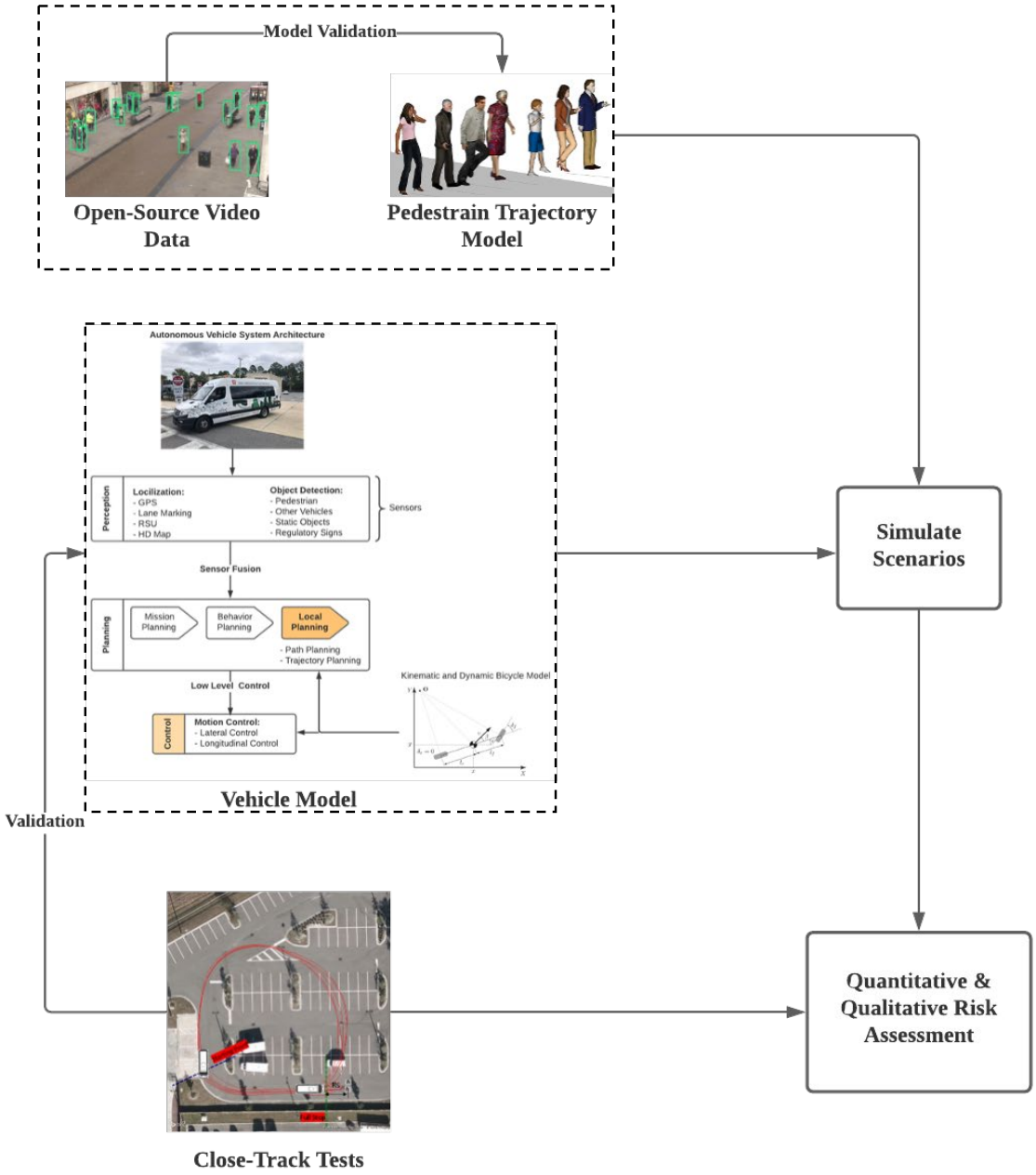

FIGURE 2: The overall research flow for LSAV-VRUs interaction

2 CLOSE-TRACK TESTS

A series of close-track tests have been conducted by our industry partner Jacksonville Transportation Authority and the shuttle performance was evaluated in different controlled scenarios. For the tested vehicle, since the autonomous

sensor stacks (Perrone Robotics) and the vehicle (GreenPower Motor Company) were manufactured by two different companies, it required extra efforts to operate the vehicle in a driverless mode. The GreenPower Company Inc. delivered the first fully autonomous EV Star transit bus to Jacksonville in collaboration with Perron Robotics on Dec 2020. The EV Star is a multi-utility vehicle capable of a range up to 150 miles (240 km).

FIGURE 3: Green Power EV Star Autonomous Shuttle Bus

The specifications of the bus are presented in TABLE 3. For developing the primary bus model, the data of the EV star bus tested by Altoona Bus Research and Testing Center have been used *(2)*. The bus operates in both autonomous and manual modes. When the bus is operating autonomously, pressing one button puts the vehicle into manual mode and the AV system will continue to run but it removes all control signals. The bus is retrofitted with a set of sensors and actuators including a camera, three Radars and Lidars, and two Global navigation satellite system (GNSS) antennas. FIGURE 4 shows the placement of each sensor on the bus.

TABLE 3: Bus Specification

Item	Description
Length × Width × Height (m)	7.42×2×2.8
Wheelbase (m)	4.32
Battery Capacity (kWh)	118 with 4 Packs
Brake system	ABS-Front disk/rear drum beak
Suspension system	McPherson independent front/ Variable cross-section longitudinal lead spring rear
Tire	215/75R17.5
ABS+EBS	Active Brake System + Electronic Brake System

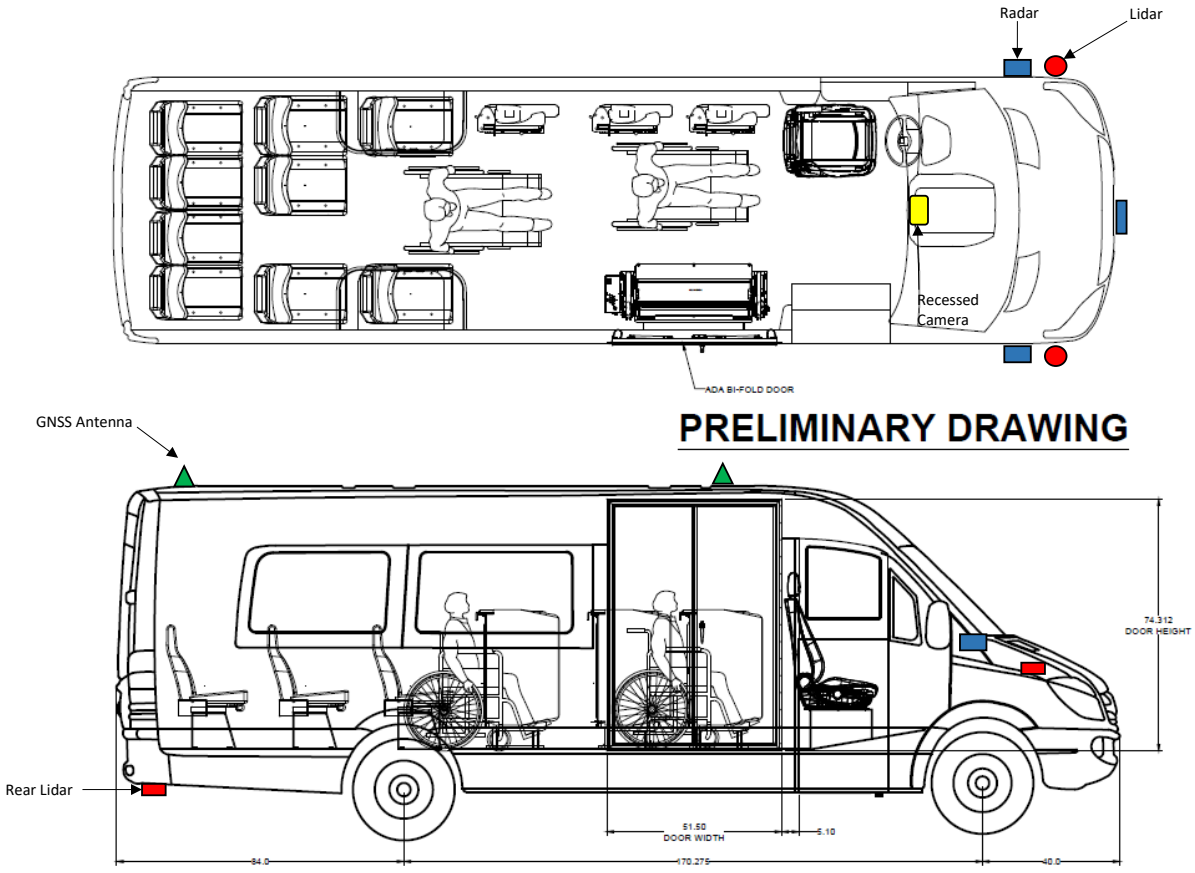

FIGURE 4: Sensor placement on the EV Star Bus provided by PerronRobotic company

2.1 TEST DATA

A total of 21 tests that are related to pedestrians and cyclists were conducted. Due to the weather condition in Florida, the heavy rain test was also conducted to have a primary evaluation on the bus performance in adverse condition. The average operational speed due to the safety consideration was between 6 mph to 13 mph. All the tests were conducted on an asphalt road and during the daytime. FIGURE 5 shows the schematic of the site that all tests were conducted.

The data of bus kinematics were recorded by two independent data acquisition systems (the VBOX provided by JTA and sensor stacks of Perron Company). For this project we used only the VBOX data that recorded the speed, acceleration, position, and orientation of the bus at each moment.

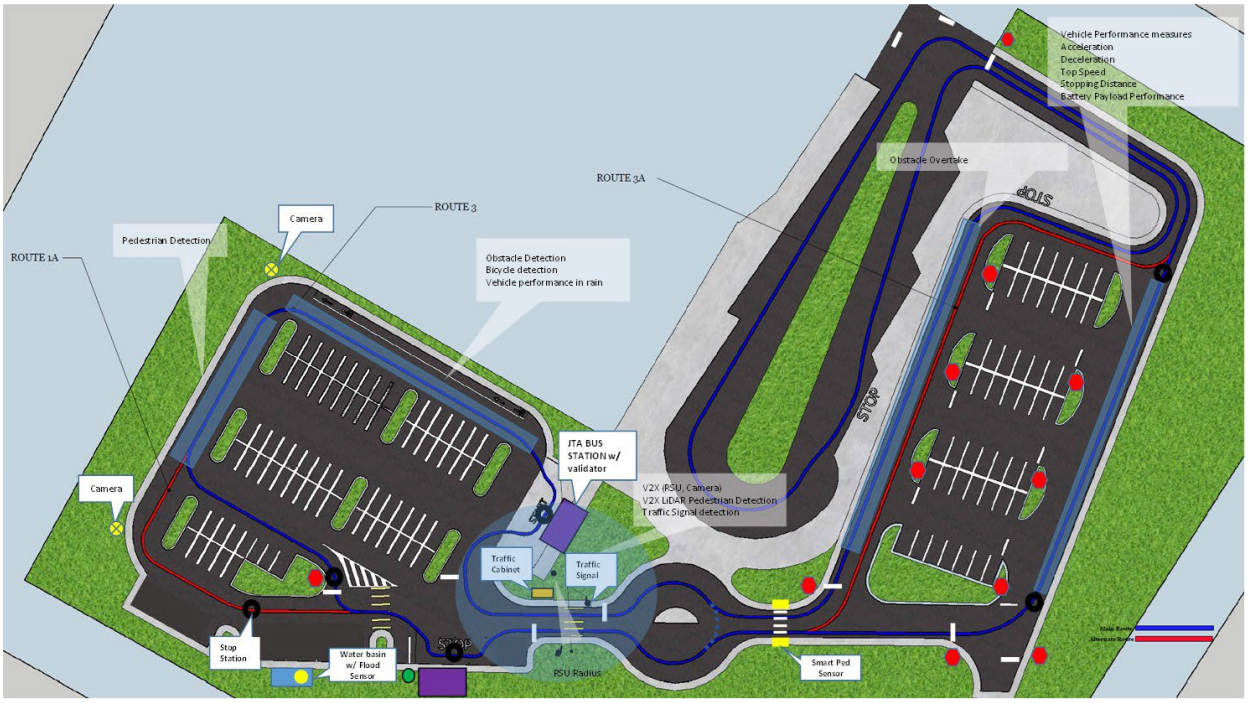

FIGURE 5: Testing site location at 3191 Armsdale Rd, Jacksonville, Florida

2.2 STATIONARY PEDESTRIAN

In the first series of tests, the basic pedestrian test using a stationary human mannequin was conducted at three different pedestrian positions relative to the driving path. The schematic of the test scenario is shown in FIGURE 6. In all tests, the nominal vehicle speed was 14.5 kph (= 9 mph). TABLE 4 shows the summary of the test results for each scenario. The average stopping distance (Rs) was 3.8 m away from the pedestrian.

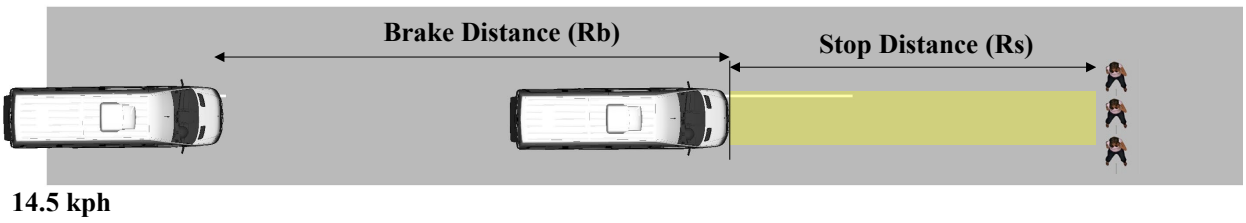

FIGURE 6: Schematic illustration of stationary pedestrian test

TABLE 4: Summary of the test results

Scenarios	Test Number	Roadway Surface	Vehicle Speed (kph; ±0.5)	Stopping Distance (m; ±0.1)
Stationary Pedestrian in the middle of the path	M1	Asphalt/Dry	14.5	4.2
	M2	Asphalt/Dry	14.5	3.7
	M3	Asphalt/Dry	14.5	4.0
Stationary Pedestrian on the left side of the path	L1	Asphalt/Dry	14.5	4.1
	L2	Asphalt/Dry	14.5	3.8
	L3	Asphalt/Dry	14.5	3.7
Stationary Pedestrian on the right side of the path	R1	Asphalt/Dry	14.5	3.7
	R2	Asphalt/Dry	14.5	3.6
	R3	Asphalt/Dry	14.5	3.7

FIGURE 7 shows the test location at the JTA Test & Learn facility. The starting point and the bus position at the full stop are marked in the aerial map view. The average time for each test was about 16 s. The yellow points in the map show the waypoints that are defined for the bus movement and the red lines are the actual bus path during each test. The final position of the bus relative to the stationary pedestrian is also shown in FIGURE 7.

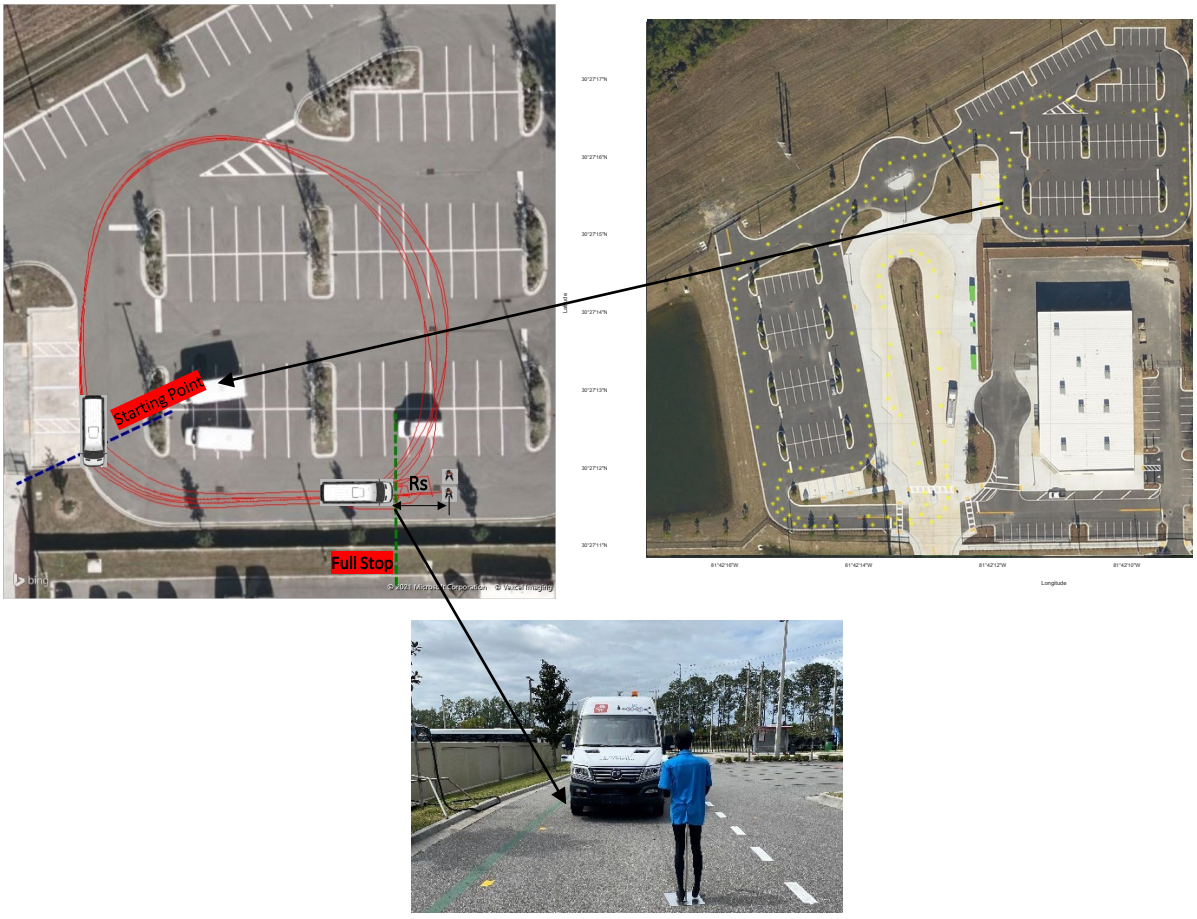

FIGURE 7: Stationary pedestrian test conducted by JTA at the Test &Learn Facility

FIGURE 8 shows the time history of the vehicle speed from the first two series of tests. The average vehicle deceleration from the tests was 0.15g and only in one case (the M3 test), the vehicle deceleration was 0.4g. To extract the braking properties of the vehicle the average braking distance (Rb) was also extracted from data, and it was equal to 5.4m.

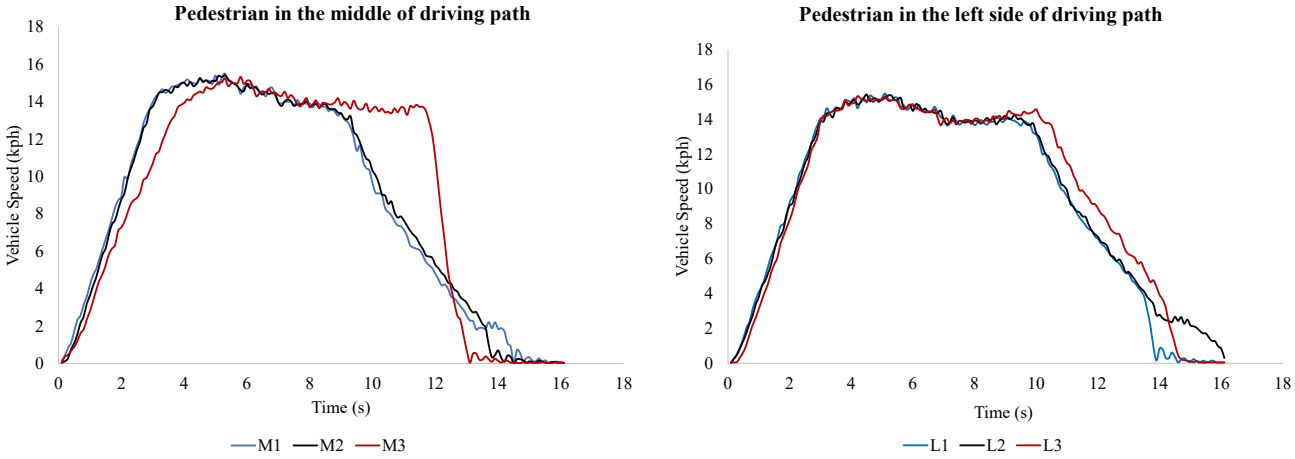

FIGURE 8: Vehicle speed time history for each test

TABLE 5 and TABLE 6 show the details of each test conducted by our industry partner during the third quarter of the project. Each test was repeated at least three times to acquire more reliable data. Besides vehicle performance, the ambient temperature, humidity, and wind speed at the beginning of each test were also recorded.

TABLE 5: Details of close-track test conditions and vehicle performance regarding pedestrian

Scenario	Test Name	Environmental Condition	Vehicle maximum speed (mph)	Note
Response to moving pedestrian 3ft away (pedestrian speed = 3 mph)	SC1-1	Temperature = 91F Humidity = 41% Wind speed = 12 mph	9	As the vehicle approached the pedestrian the vehicle made a lane adjustment and proceeded pass at a reduced speed.
	SC1-2			As the vehicle approached the pedestrian the vehicle made a lane adjustment and proceeded pass at a reduced speed.
	SC1-3			As the vehicle approached the pedestrian the vehicle made a lane adjustment and proceeded pass at a reduced speed.
Pedestrian Detection Test for different pedestrian positions (stationary): SC6: Existing Crosswalk	SC6-1	Temperature = 70-72F Humidity = 99% Wind speed = 5 mph	6	The vehicle detected a pedestrian slowed adjusted positioning in its lane and came to a stop in the crosswalk with the front bumper just passed the pedestrian.
	SC6-2			The vehicle detected a pedestrian slowed adjusted positioning in its lane and came to a stop in the crosswalk. The vehicle came to a stop before it reached the pedestrian.
	SC6-3			Vehicle detected pedestrian slowed adjusted positioning in its lane. The vehicle hesitated as it approached the pedestrian but continued to proceed through the crosswalk pass the pedestrian.

SC5: Mid-Lane	SC5-1	Temperature = 72F Humidity = 91% Wind speed = 9 mph	6	Detected pedestrian, adjusted positioning in its lane slowed and came to a stop.
	SC5-2			Detected pedestrian, adjusted positioning in its lane slowed and came to a stop.
	SC5-3			Detected pedestrian, adjusted positioning in its lane slowed and came to a stop.
SC4: Entering Crosswalk	SC4-1	Temperature = 73F Humidity = 13% Wind speed = 6 mph	6	Vehicle detected pedestrian, reduced speed, made lane adjustment, hesitated and then proceeded past the pedestrian.
	SC4-2			Vehicle detected pedestrian, reduced speed, made lane adjustment, hesitated and then proceeded past the pedestrian. During the adjustment, the vehicle started to make the left turn before the actual programmed turn was to occur.
	SC4-3			Vehicle detected pedestrian, reduced speed, made lane adjustment, hesitated and then proceeded past the pedestrian. During the adjustment, the vehicle started to make the left turn before the actual programmed turn was to occur.

TABLE 6: Details of close-track test conditions and vehicle performance for heavy rain and cyclist test

Scenario	Test Name	Environmental Condition	Vehicle maximum speed (mph)	Note
Rain Test	SC1-R1	Temperature = 73F Humidity = 95% Wind speed = 6 mph	5	As the vehicle approached the pedestrian the vehicle made a lane adjustment and proceeded pass at a reduced speed.
	SC1-R2			As the vehicle approached the pedestrian the vehicle made a lane adjustment and proceeded pass at a reduced speed.
	SC1-R3			As the vehicle approached the pedestrian the vehicle made a lane adjustment and proceeded pass at a reduced speed.
Detect and Respond to Bicycle: SC5: Cyclist at Load-Side of Vehicle	SC5-B1	Temperature = 70F Humidity = 57% Wind speed = 9 mph	9	The vehicle detected cyclist and adjusted its lane position as it was approaching cyclists. The vehicle did not deviate from its projected path as it was passing cyclist. No speed change passing cyclist
	SC5-B2			The vehicle detected cyclist and adjusted its lane position as it was approaching cyclists. The vehicle did not deviate from its projected path as it was passing cyclist. No speed change passing cyclist
	SC5-B3			The vehicle detected cyclist and adjusted its lane position as it was approaching cyclists. The vehicle did not deviate from its projected path as it was passing cyclist. No speed change passing cyclist
SC8: Cyclist at Driver-Side of Vehicle	SC8-B1	Temperature = 70F Humidity = 57% Wind speed = 9 mph	9	Vehicle slowed as it was passing cyclist and then continued route at normal speed
	SC8-B2			Vehicle slowed as it was passing cyclist and then continued route at normal speed
	SC8-B3			Vehicle slowed as it was passing cyclist and then continued route at normal speed

According to the test results, no unexpected behavior or deviations from normal driving situations was observed during the tests. The purpose of these tests was to evaluate the basic performance of the LSAV, but not validating or verifying the automated systems or expanding the ODD of the automated shuttle bus. For the moving pedestrian test, in all three scenarios, the vehicle behaves similarly and passed the pedestrian at the safe distance. The test parameters were limited to only one pedestrian speed and direction. No changes in vehicle performance were observed for the same set of tests. For the stationary pedestrian tests, three positions of the pedestrian have been defined, and only when the pedestrian was located in the middle of the road the bus came to a full stop. In the two other scenarios where the pedestrian enters or exits the crosswalk, the vehicle adjusts its speed and passed the pedestrian at a specific distance.

The test environment was designed in a very conservative framework due to the safety restriction. Therefore, the safe performance of the bus during the tests does not guarantee the safe operation in another set of environments. To establish the operational design domain boundaries for this vehicle, rigorous validation tests for different safety cases are required. Currently, this can be achieved by using different techniques including a close-track site, on-road test, and modeling simulation. Each technique offers a multifaceted testing architecture with varying degrees of test control and fidelity and must be conducted at a different level of development and deployment *(3)*. For example, the company that provided the sensor stacks must ensure the functional and operational safety of those systems.

3 COMPONENTS OF THE SIMULATION FRAMEWORK

The simulation process consisted of the following four major components: 1) The vehicle dynamics model that replicates the longitudinal vehicle motion; 2) The pedestrian model that simulates the pedestrian trajectory and crossing decision; 3) The planning algorithm that determines the actions that vehicle must take at each moment based on relative distance, speed, and acceleration of vehicle and road users; 4) The control module that specifies the exact amount of acceleration or deceleration that vehicle can have based on its dynamic characteristics. FIGURE 9 shows the modeling part that will be used in this project for a different set of parameters. Each of these components has been developed in MATLAB software using a set of assumptions and simplifications due to many different reasons such as data availability and computational cost. MATLAB Simulink software was used to integrate all four modules and visualize the LSAV-VRU interaction. In the proposal stage PC-Crash software was considered, but it was changed to Matlab due to the better suitability for this project.

Each component consisted of certain input and output ports and predefined parameters within each block which interact with each other within a loop. At the beginning of the simulation (t = 0s), the required pedestrian and vehicle model uses the initial conditions such as initial position and speed. As the simulation goes forward, the vehicle dynamic model sends the vehicle position and speed to the pedestrian block at each time step (0.01s - 0.001s). The pedestrian model then uses these parameters and predefined parameters such as destination point and type of the pedestrian (reckless or cautious) to predict the pedestrian position and speed for the next time step.

The planning algorithm uses the information of relative position and speed of vehicle and pedestrian to make proper decisions in order to avoid any collision/conflict, and then set the proper command for the control module. The

controller will then use the new reference speed, and the current speed of the vehicle to apply proper acceleration/deceleration to the vehicle block.

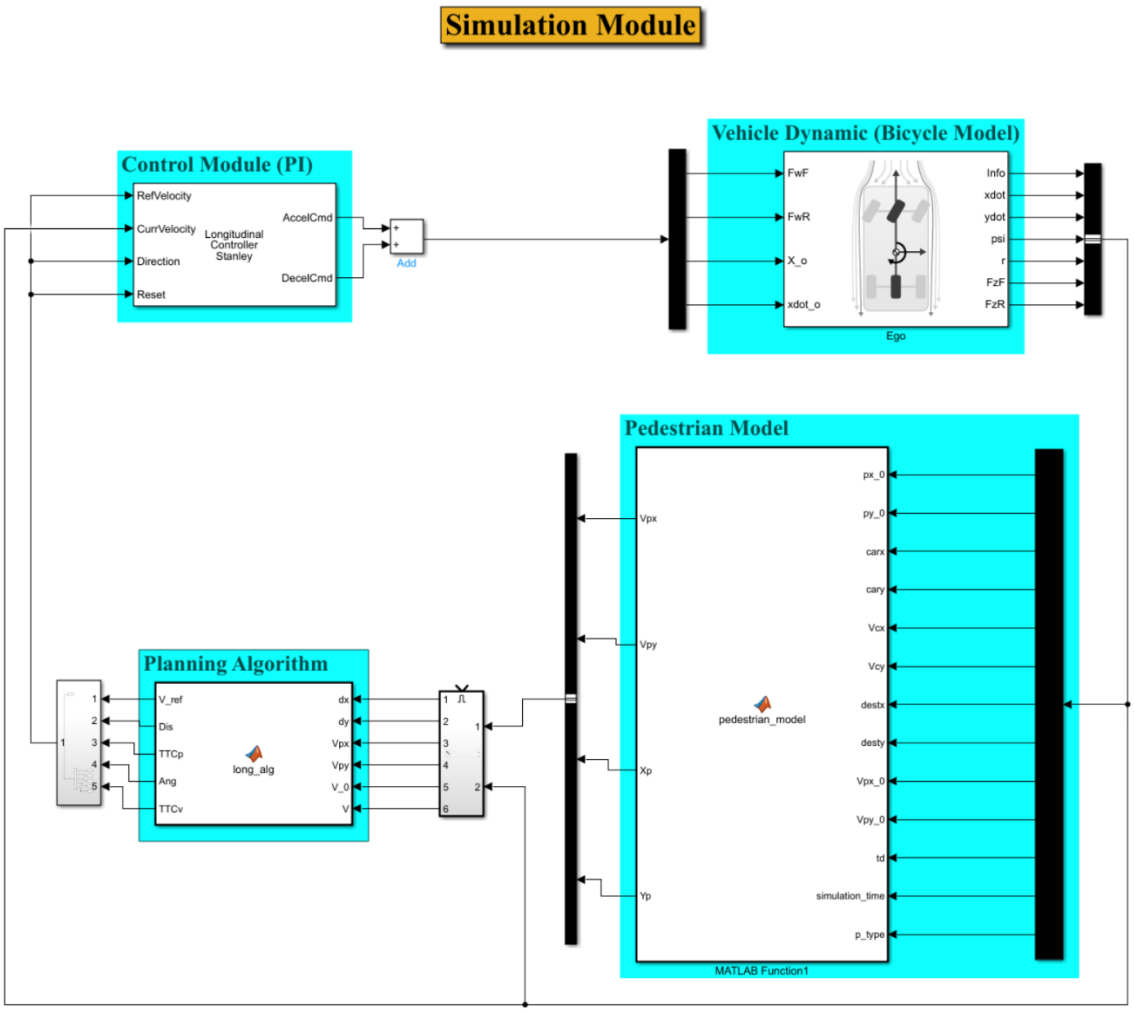

FIGURE 9: The framework of the MATLAB simulation for the LSAV-VRU interaction

To account for the variability of sensor stacks in different LSVs, the level of simulation complexity of LSAV has been adjusted accordingly. For example, the sensor stack for the currently tested LSV has been provided by PerrornRobotic which has different sensor architecture and detection algorithms than other types of LSAV such as Olli (Local Motors). In our simulation process, we defined the pedestrian detection error that was associated with these detection modules ranging from 2 to 5 % *(4)*. The detection accuracy of the system also depends on environmental factors and traffic conditions such as time of the day, weather conditions (rainy, fog etc.), the reflection of the road surface, and occlusion of other vehicles. In this project, since the LSAV was only tested in a controlled set of environmental conditions, it was not feasible to obtain information about the actual performance of the detection system under actual operational conditions. Therefore, we implemented the results of previous studies to some extend *(5)*. Additionally, the pedestrian behavior model was developed to have a more realistic assessment. The details of the simulation process for each component are explained in the following sub-sections.

3.1 VEHICLE DYNAMIC MODEL

In this section, the vehicle model used for simulating vehicular motion is discussed. The most widely used models are the bicycle dynamic model and bicycle kinematic model (see FIGURE 10). TABLE 7 shows their application, the assumptions for each model, and their limitations. The vehicle data extracted from the actual test was used to check which model performs well in our application.

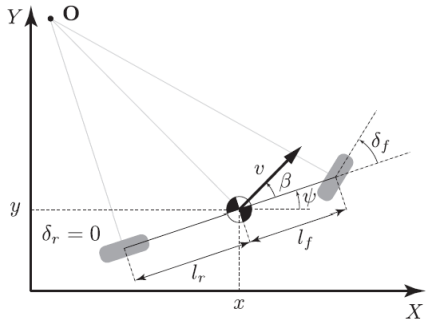

FIGURE 10: The bicycle model of the vehicle *(6)*

TABLE 7: Vehicle Models for path planning and motion control *(6)*

Item	**Kinematic Bicycle Model (based purely on vehicle's geometric relationships)**	**Dynamic Bicycle Model (take mass, inertia, tire stiffness, and road friction into consideration)**
Equations	$\dot{x} = v\cos(\psi + \beta)$ $\dot{y} = v\sin(\psi + \beta)$ $\dot{\psi} = \frac{v}{l_r}\sin(\beta)$ $\dot{v} = a$ $\beta = \tan^{-1}(\frac{l_r}{l_f + l_r}\tan(\delta_f))$	$\ddot{x} = \dot{\psi}\dot{y} + a_x$ $\ddot{y} = -\dot{\psi}\dot{y} + \frac{2}{m}(F_{c,f}\cos\delta_f + F_{c,r})$ $\ddot{\psi} = \frac{2}{I_z}(l_f F_{c,f} - l_r F_{c,r})$ $\dot{X} = \dot{x}\cos\psi - \dot{y}\sin\psi$ $\dot{Y} = \dot{x}\sin\psi - \dot{y}\cos\psi$
Notations	x and y: coordinates of the center of mass, $\dot{x}$ and $\dot{y}$: longitudinal and lateral speeds ψ: inertial heading angle v: vehicle speed l_f and l_r: distances from rear and front axles β: angle of the current velocity a: vehicle acceleration	m and I_z: vehicle's mass and yaw inertia $F_{c,f}$ and $F_{c,r}$: lateral tire forces for front and rear wheel δ_f: steering angle
Assumption	Vehicle does not slip (true for low-speed vehicles)	
Limitation	– Steering change can be unrealistic and needs to be constrained using steering angle change rate	– The tire model becomes singular at low speed – Computationally expensive,
Application	– Path planning at low speed where inertial effects is small	– Design control systems

FIGURE 11 shows the general information that was used for the vehicle dimension, weight distribution, and suspension properties.

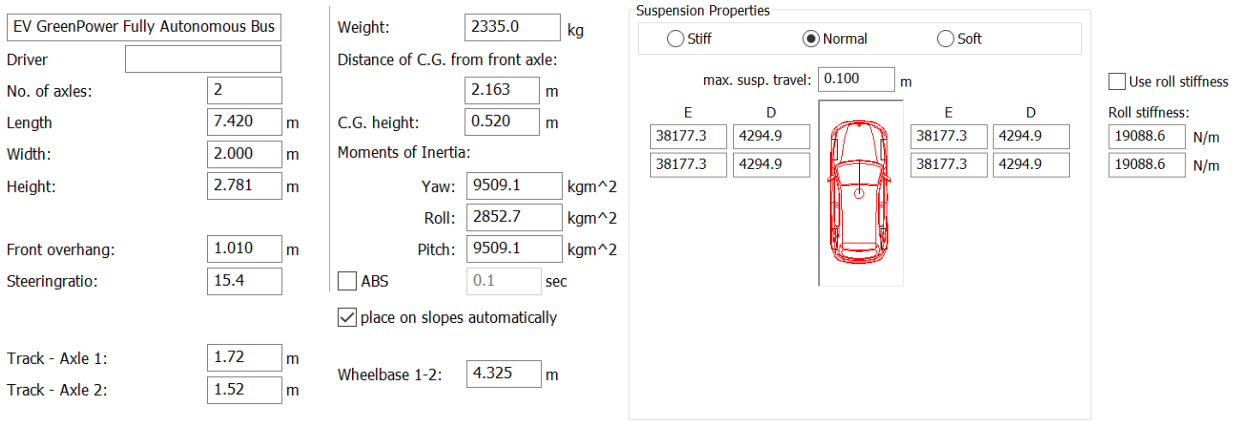

FIGURE 11: Vehicle properties used for simulation

3.2 PLANNING AND CONTROL

FIGURE 12 illustrates the safe distance that a vehicle must keep at all operational situations from the pedestrian. The space around the vehicle is divided into two regions: 1) A collision zone that has the highest of crashes and the pedestrian cannot enter in this region to ensure traffic safety; 2) A conflict zone where the pedestrian may feel unsafe to be around. The vehicle speed before it enters the active region is kept as constant. When the vehicle enters the active region, it adjusts speed to keep the safe distance from the pedestrian. A safe zone around the pedestrian is used which is circular in shape. The length of active region depends on the speed of the car and time to collision (TTC). TTC is one of the surrogate safety parameters that has been used widely to evaluate safety performance *(7)*.

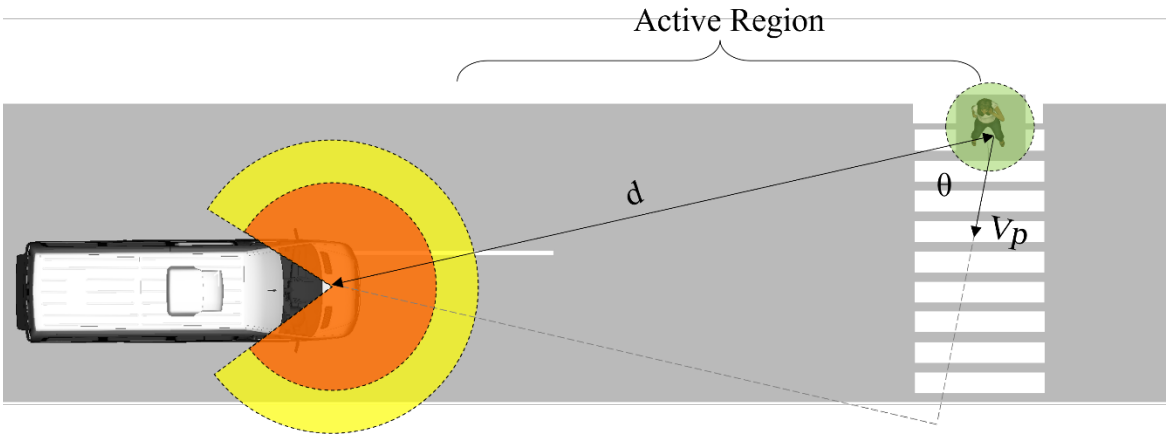

FIGURE 12: The vehicle and pedestrian boundaries

The collision zone, conflict zone, and active region are the parameters that can be varied depending on the type of safety algorithms used in LSAVs design. Also, the lateral safe distance of the vehicle has another constraint

that is related to its driving path width. This means that the vehicle can only deviate from its original path within certain range and if the maneuver causes a risk of crash for other agents, the vehicle must slow down and come to full stop. Therefore, different traffic conditions and roadways can change the vehicle path to minimize the risk of any conflict with the pedestrian. These are considered as edge cases that the vehicle systems must be tested and validated against to ensure the safety of vehicle operations.

The maximum allowable acceleration and deceleration for the LSAV must also be defined in the control module. Due to the lack of access to this information the average value that a typical vehicle can have for these two parameters has been selected. The maximum deceleration of -5 m/s^2 and maximum acceleration of 6 m/s^2 were used for simulations. The controller was implemented as a discrete Proportional-Integral (PI) controller with integral anti-windup.

For addressing the detection error of sensors in the autonomous vehicle, three types of sensors are used. Based on the error percentage of detection, the dynamics of vehicle can be changed such as variation of speed, acceleration or deceleration to avoid hitting the pedestrian. The error percentage of different types of sensors are shown in TABLE 8.

TABLE 8: Types of sensors

Sensor type	Percentage of error (%)
1	0 - 3
2	0 - 5
3	0 - 10

3.3 PEDESTRIAN MOTION MODEL

3.3.1 INTRODUCTION

Pedestrians are considered as vulnerable road users because they are directly exposed in the road network to vehicles and chances of collision and injury risk are very high. In a road network, vehicle motion is restricted in the longitudinal direction inside traffic lanes, and it cannot move suddenly in the lateral direction. Unlike the trajectory of vehicles, pedestrians can change their moving direction frequently and they can make their own decision while interacting with vehicles. FIGURE 13 shows the factors that influence pedestrian behavior which is classified into two main categories of pedestrian and environmental factors *(8)*.

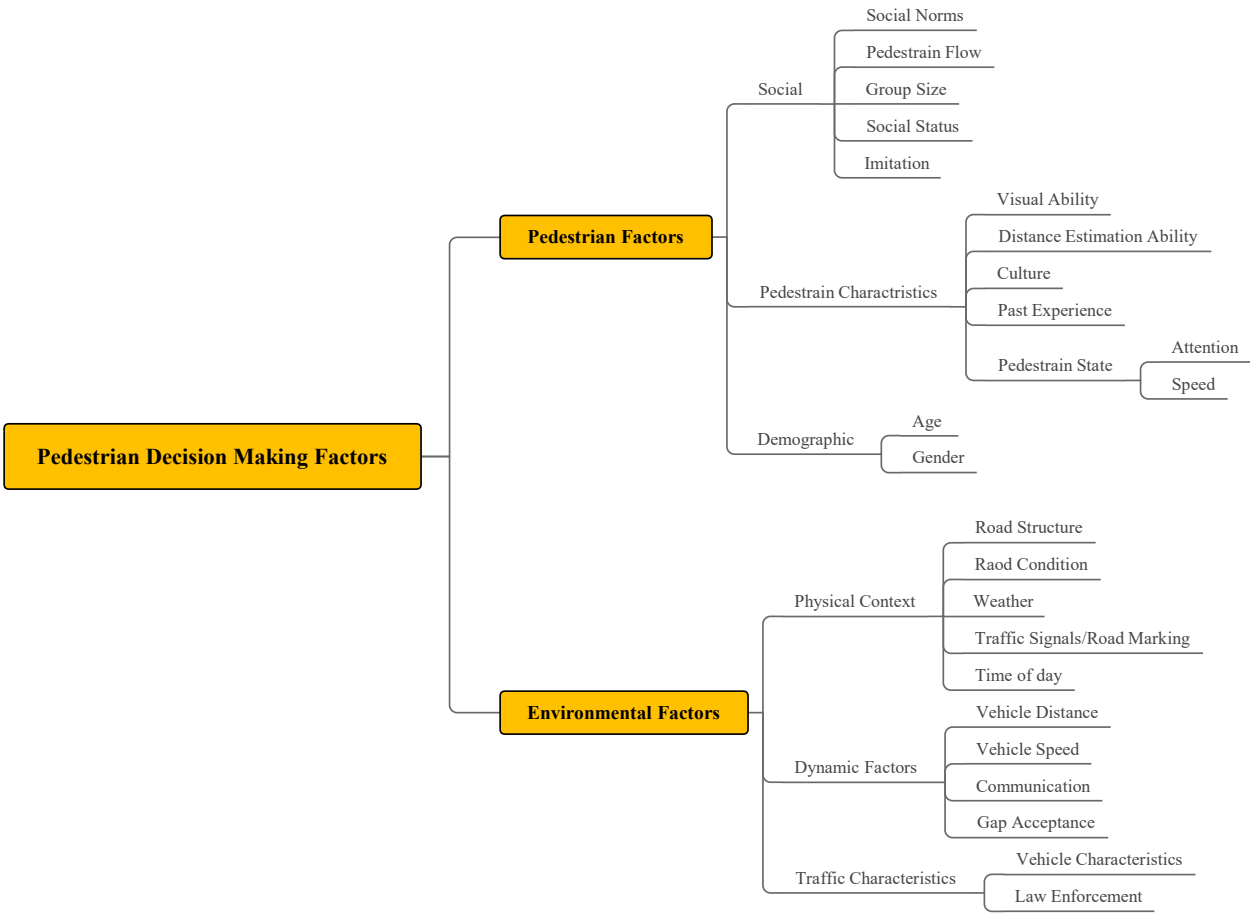

FIGURE 13: Factors influencing pedestrian behavior *(8)*

Behavior of pedestrian has been studied and intention estimation has been conducted to predict the pedestrian's motion in the short-term (1-2.5 seconds) and long-term (final destination or path following) *(9)*. For the short-term approach, researchers are using the pedestrian's head orientation, body movement, and the potential impacts of social factors. In the long-term approach, researchers usually draw information from static cameras or lidars *(10)*. They have mostly used questionnaires or interviews to obtain the information needs of VRUs who encounter LSAVs *(11)*. Some of the findings of recent studies have been highlighted as follows:

- People prefer to have separate path/pavement in the driverless environment (based on a questionnaire) *(12)*
- On average, cyclists do not expect to be recognized better by the LSAVs (based on photo experiments) *(13)*
- Pedestrians feel less safe when approaching a driver-less car (based on field experiment) *(14)*
- People tend to cross the street at the vehicle's deceleration phase, rather than after it had come to a full stop (based on virtual reality-based simulation) *(15)*
- Prediction of waiting was harder than a prediction of crossing behavior (based on experimental and real-traffic data) *(16)*

Researchers have studied the application of smart infrastructure, external human-machine interfaces, and the potential of augmented reality to overcome these challenges *(17)*. They have found the key role of smart infrastructure in solving this challenge and suggested the LSAV-VRUs segregation might be also needed for future urban areas. However, they were concerned about corresponding costs and maintenance requirements *(17)*.

Walking speed is one of the main characteristics of the pedestrian that depends on various contextual and individual variables. There have been several studies to quantify the walking speed and how parameters influence the rate of speed. These studies have used field observation, manual video, and semi-automated video analysis methods to characterize the kinematics of pedestrians *(18)*. The average walking speed resulted from those studies ranged from 0.7 m/s to 1.3 m/s in different traffic conditions.

Predicting pedestrian trajectory while interacting with a surrounding vehicle can help in developing algorithms for the autonomous vehicle. To simulate the pedestrian trajectory, several motion models have been used. Among them, the social force model (SFM) uses differential equations by combining different attractive and repulsive forces acting on pedestrians. This model was proposed initially for pedestrian-pedestrian interaction by Helbing and Molnar *(19)*. Since then, it has been modified by several researchers to integrate pedestrian-vehicle interaction for the development of autonomous vehicle algorithms.

3.3.2 INTERACTION SCENARIOS

Two scenarios were considered for the simulation of LSAV-VRU interactions. The first scenario is the crossing at a crosswalk and the second scenario is the crossing at a roundabout. FIGURE 14 and FIGURE 15 illustrate the scenarios that were used to conduct the simulation of interaction framework. In the scenarios we analyzed, a pedestrian was trying to move into a continuous space while interacting with an autonomous vehicle. SFM was applied to this pedestrian (referred to as 'ego pedestrian'). Ego pedestrian will go from starting point to a fixed destination and try to use the shortest available path without deviating too much. The goal is to predict the trajectory of ego pedestrians without colliding with AV. According to SFM, an attractive force known as destination force will be used which guides ego pedestrian towards the destination. During navigation, ego pedestrians will also face repulsive forces coming from AV.

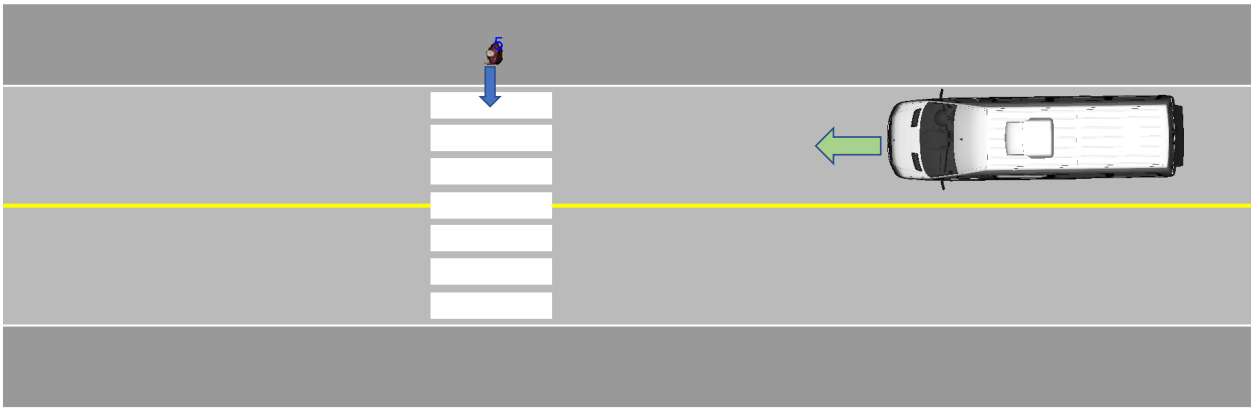

FIGURE 14: Crosswalk scenario

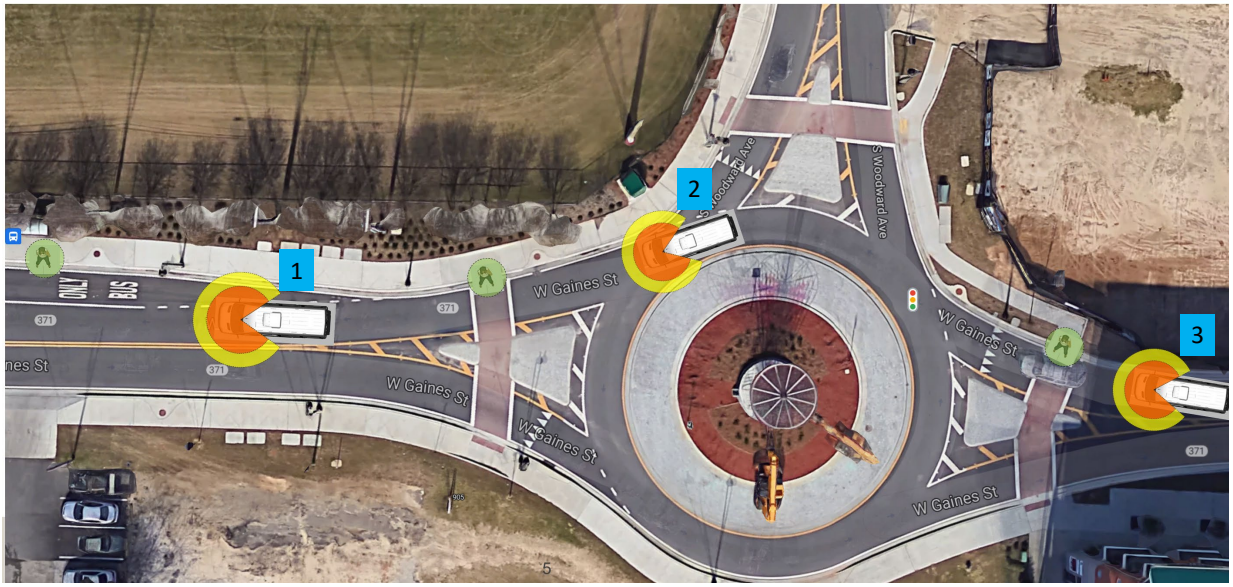

FIGURE 15: Roundabout scenario

3.3.3 SOCIAL FORCE MODEL (SFM)

A microscopic social force model was used to simulate pedestrian trajectory while interacting with a vehicle. In the following, the equations given in Anvari et al. *(20)* for pedestrian motion simulation by SFM are summarized. Three types of forces act on a single pedestrian, and they are added together to produce the pedestrian trajectory. These forces can be referred to as a destination force, a repulsive force from a vehicle, and random fluctuation force shown in Eq. 1.

$$\boldsymbol{F}_{total}(t) = \boldsymbol{F}_d(t) + \boldsymbol{F}_v(t) + \boldsymbol{F}_e(t) \quad (1)$$

Here, $\boldsymbol{F}_d$ is a destination force that drags a pedestrian from a starting point towards the destination point, $\boldsymbol{F}_v$ is a repulsive force coming from a vehicle that enables pedestrians to keep a certain distance away from the vehicle for safe navigation, and $\boldsymbol{F}_e$ is a random fluctuation force. Destination force can be expressed by Eq. 2.

$$\boldsymbol{F}_d(t) = \frac{v^0 \boldsymbol{e}^0 - \boldsymbol{v}}{\tau} \quad (2)$$

Here, v^0 is a comfortable walking velocity that motivates the pedestrian to move in the desired direction $\boldsymbol{e}^0$ within a certain relaxation time τ. The desired direction $\boldsymbol{e}^0$ is a unit vector that points from a pedestrian current location to a fixed destination point and $\boldsymbol{v}$ is pedestrian speed. The repulsive force coming from a pedestrian is shown in Eq. 3.

$$\boldsymbol{F}_v(t) = A_v \exp^{\frac{r_v + r_p - d_{vp}}{B_v}} \boldsymbol{e}^{vp} F_{vp} \quad (3)$$

Here, A_v and B_v are constants, r_v is the radius of vehicle, r_p is the radius of pedestrian, d_{vp} is the distance between a pedestrian and a vehicle, $\boldsymbol{e}^{vp}$ is a unit vector that denotes the direction of a repulsive force coming from the vehicle to the ego pedestrian and F_{vp} is used to denote the effective field view of pedestrian towards the vehicle. The shape of the vehicle used in the SFM is considered as an ellipse with a radius r_v. The value of r_v is dependent on the angle ($\emptyset_{pv}$) between the walking direction of the pedestrian and a line that connects the center points of both pedestrian and vehicle. The equation to calculate $\mathrm{r_v}$ is shown in Eq. 4.

$$r_v = \frac{w_v}{\sqrt{1-\epsilon^2\cos^2(\emptyset_{pv})}}, \text{where } \epsilon = \frac{\sqrt{{l_v}^2-{w_v}^2}}{l_v} \quad (4)$$

Here, $2l_v$ and $2w_v$ are the length and width of the vehicle respectively. FIGURE 16 shows the diagram that is used for calculating the radius of vehicle r_v.

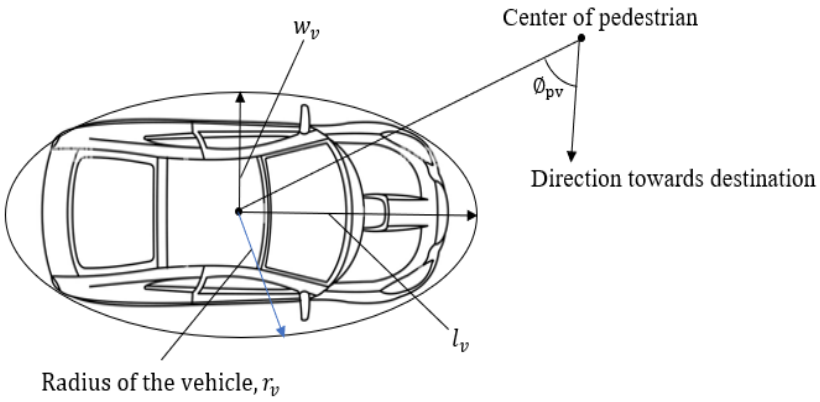

FIGURE 16: Radius of the elliptical shape of the vehicle

The equation for calculating the effective field of view F_{vp} is shown in Eq. 5. Here, λ is a constant that influences the field of view.

$$F_{vp} = \lambda + (1-\lambda) \times \frac{1+\cos(\emptyset_{pv})}{2} \quad (5)$$

The random fluctuation force is expressed by Eq. 6.

$$\boldsymbol{F}_e(t) = \text{dot}\big(\boldsymbol{e}^0(t), \boldsymbol{F}_{total}(t)\big) X\, \boldsymbol{e}^{norm}(t) \quad (6)$$

Here, X is a random variable that follows a normal distribution with a mean of 0 and a standard deviation of 1. $\boldsymbol{e}^{norm}$ is a unit vector tangential to the desired direction $\boldsymbol{e}^0$. After calculating the total force acting on the ego pedestrian, the velocity and position are calculated and updated for each time step and the pedestrian trajectory is formed.

To address the crossing decision behavior, a gap acceptance model is used. Time to collision (TTC) can be used as a benchmark for deciding whether an allowable time gap is accepted by a pedestrian before crossing. Based on the initial position of both vehicle and pedestrian, a conflict point is selected if both agents start moving and do not deviate from their trajectories. The time required to reach the conflict point is calculated for both agents by using initial conditions of the first-time step of simulation. For calculating the TTC, the distance between pedestrian and vehicle is used because the distance influences the gap acceptance behavior of the pedestrian *(21)*. If the time to reach the conflict point for pedestrian is less than the time required for the vehicle, the pedestrian starts to cross the road and vice versa. The equations used for TTC of both pedestrian and vehicle is given in Eq. 7 and Eq. 8 respectively.

$$TTC_{pedestrian} = \left|\frac{y_{pedestrian} - y_{vehicle}}{v_{y,pedestrian}}\right| \quad (7)$$

$$TTC_{vehicle} = \left|\frac{x_{pedestrian} - x_{vehicle}}{v_{x,vehicle}}\right| \quad (8)$$

Here, $TTC_{pedestrian}$ can be varied based on individual pedestrian characteristics that reflects the risk acceptance level *(22)*. According to Das et al. *(23)*, the minimum accepted time gap before crossing is two seconds and the mean

accepted time gap is eight seconds. For this project, three types of pedestrians were considered based on the time to collision to reflect the difference in risk-taking attitude during crossing. TABLE 9 shows the types of pedestrians used in the simulation framework and their accepted TTC. A distracted pedestrian does not stop during crossing; for example, a person who is using cellphone and does not look at road. Risk-taker pedestrian tries to cross the road before vehicle arrives unless it is too risky to cross and accepts the TTC of two seconds. A cautious pedestrian considers the vehicle position before starting to cross and maintains a safe distance greater than the risk-taker pedestrian and a TTC value of five seconds is selected for the cautious pedestrian.

TABLE 9: Types of pedestrians considered for simulation

Pedestrian type	Accepted time to collision (TTC)
Distracted	0s
Risk-taker	2s
Cautious	5s

3.3.4 VALIDATION OF SOCIAL FORCE MODEL

For validating the simulated trajectory obtained from the social force model, we use the Control and Intelligent Transportation Research (CITR) dataset collected by Yang et al. *(24)*. They conducted controlled experiments in a parking lot at the Ohio State University. The layout of their experiment area is shown in FIGURE 17. The researchers used a DJI Phantom 3 SE Drone with a down-facing camera for video recording. The video resolution is 1920×1080 with a fps of 29.97. During the experiments, participants were instructed only to walk from one small area (starting points) to another small area (destinations). They used an EZ-GO Golf Cart that interacts with surrounding pedestrians, as shown in FIGURE 17.

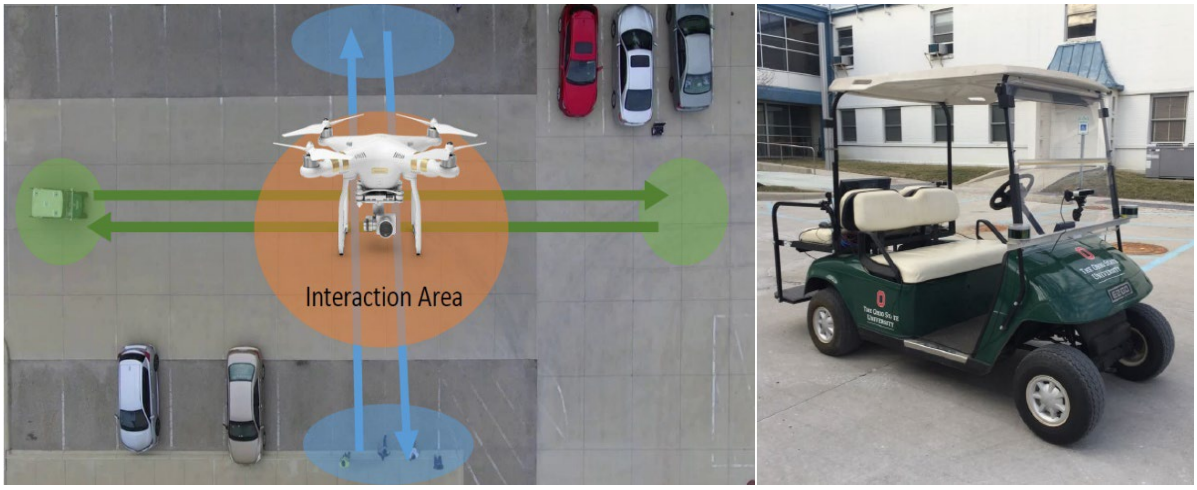

FIGURE 17: Layout of controlled experiment area of CITR dataset and EZ-GO Golf Cart *(24)*

We consider two cases for the pedestrian trajectory simulation from the CITR dataset: vehicle yields to a crossing pedestrian and vehicle does not yield to a crossing pedestrian. Trajectories of the pedestrian and vehicle were extracted from the CITR dataset and used in simulation. TABLE 10 shows the initial speed of the pedestrian and pedestrian number for each scenario. The vehicle trajectory is extracted from the CITR dataset.

TABLE 10: Summary of input parameters

Scenario Number	1			2		
Pedestrian Number	P1	P2	P3	P1	P2	P3
Pedestrian Initial Speed (m/s)	1.4	0.8	0.6	1.1	1.5	1.25

FIGURE 18 and FIGURE 19 show the pedestrian trajectories from the actual dataset and our simulation models for scenario 1. The results indicate that the pedestrian model was able to predict the trajectory. Although the pedestrian motion prediction is a very complicated task that requires the physical and phycological information of each individual, for this project the model can provide sufficient results. Similarly, FIGURE 20 and FIGURE 21 show the pedestrian trajectories for scenario number two where the vehicle did not yield to the pedestrian.

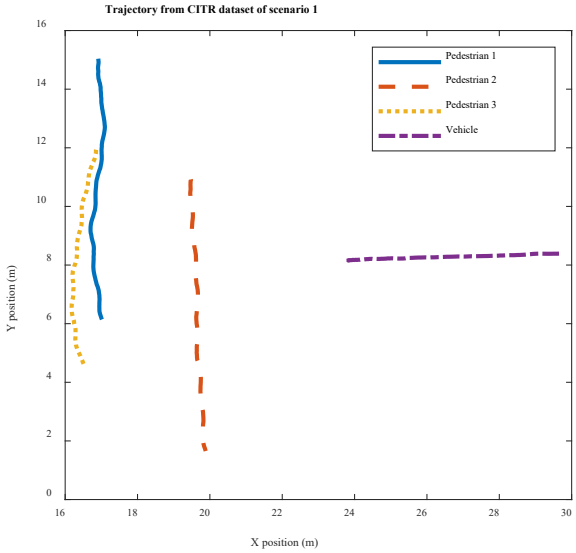

FIGURE 18: Trajectories extracted from the CITR dataset *(24)*: scenario 1

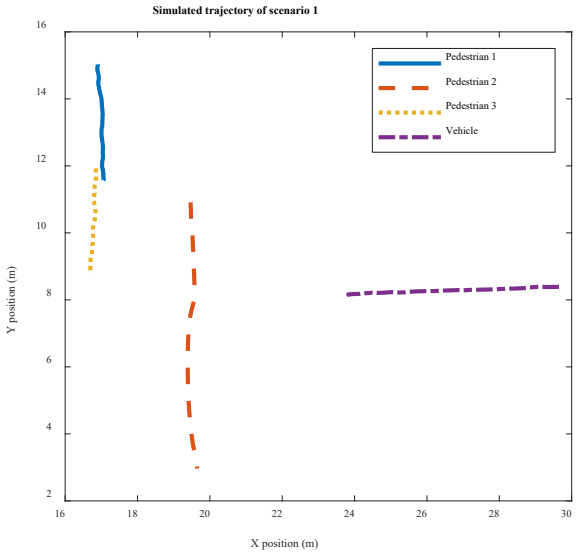

FIGURE 19: Trajectories resulted from simulation: scenario 1

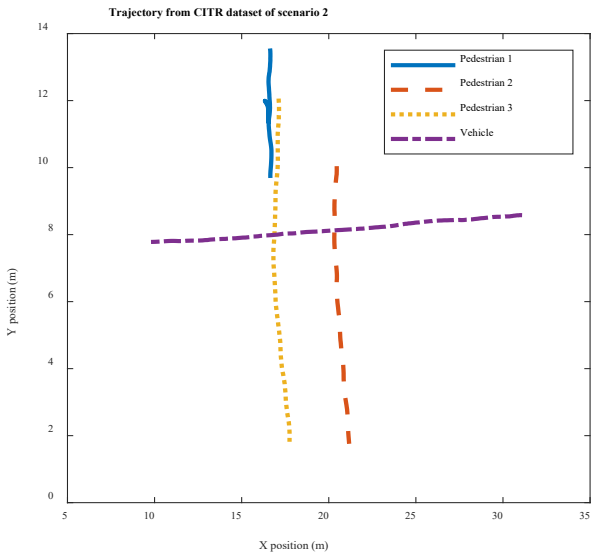

FIGURE 20: Trajectories observed from the CITR dataset *(24)*: scenario 2

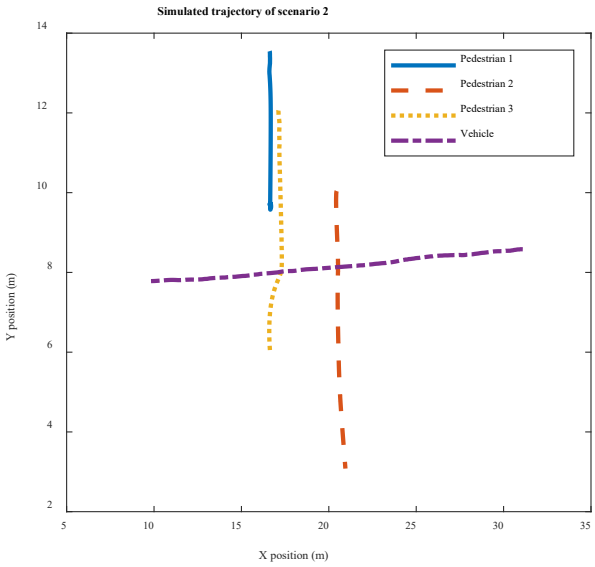

FIGURE 21: Trajectories resulted from simulation: scenario 2

Further simulations were conducted to illustrate the trajectory of a single pedestrian trying to cross. The input parameters used for simulation are provided in TABLE 11. We have selected 1.5 m/s initial velocity as it is average pedestrian crossing velocity found in study in Florida *(25)*. We divided the total time of simulation (T) into 5 sub-divisions (0, 0.25T, 0.5T, 0.5T, and T). Total time of simulation is denoted as T. We added another timestep called 'stop time' to demonstrate pedestrian stopping position when the vehicle did not stop (scenario 2) as shown FIGURE 23. The pedestrian paused for a brief time when the time gap between the pedestrian and the vehicle was less than the critical time gap. A timestep called 'stop time' was added to demonstrate the position of both pedestrian and vehicle when the pedestrian paused but the vehicle was moving. After the time gap value became higher than the critical gap, the pedestrian started crossing again. In FIGURE 22, the vehicle stopped to let the pedestrian cross (scenario 1). The SFM was able to generate realistic pedestrian trajectories during the crossing.

TABLE 11: Input parameters for simulating the pedestrian trajectory at different timesteps

Scenario Number	Pedestrian Initial Position	Pedestrian Destination	Pedestrian Initial Speed (m/s)	Vehicle Initial Position	Vehicle Destination	Vehicle Initial Speed (m/s)
1	18.35, 11	18.95, 2.95	1.5	29.65, 8.38	23.84, 8.15	1.96
2	17.12, 12.06	17.74, 1.82	1.5	31.09, 8.58	9.58, 7.78	2.19

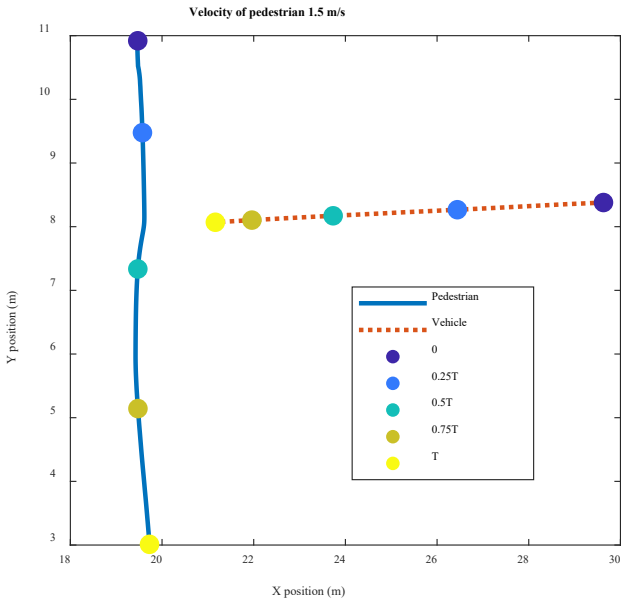

FIGURE 22: Simulated trajectory with pedestrian velocity 1.5 m/s: scenario 1

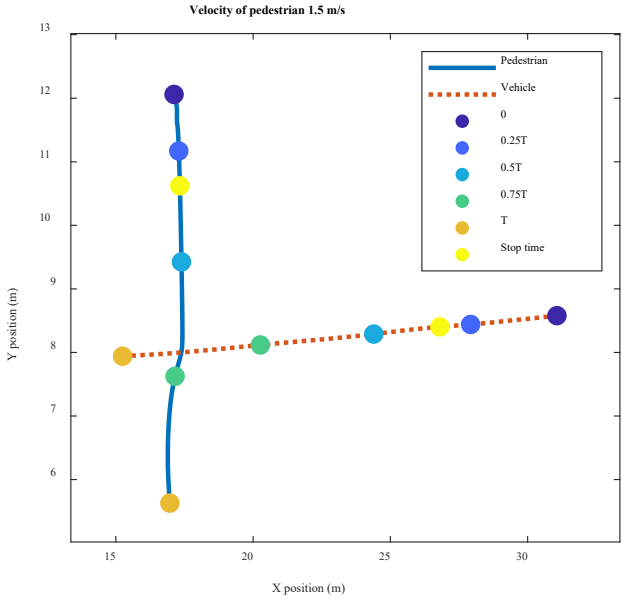

FIGURE 23: Simulated trajectory with pedestrian velocity 1.5 m/s: scenario 2

3.4 SIMULATION RESULTS

3.4.1 INPUT PARAMETERS

For simplicity, the initial position of vehicle and pedestrian were fixed for each simulation. A total of 1000 simulations were conducted for the crosswalk scenario with different initial input parameters to account for the variability of pedestrian behavior. Among the 1000 simulations, 200 was done for cautious pedestrian, 400 was done for risk-taker, and the remaining 400 was done for distracted pedestrians. For the roundabout scenario, a total of 200 simulations were conducted where 32 was done for cautious pedestrian, 90 was done for risk-taker and 78 was done for distracted pedestrians. The focus of this simulation work was to simulate more risky interactions between AV and pedestrian, and as a result fewer simulations were conducted for cautious pedestrians than other two types of pedestrians.

According to Knoblauch et al. *(25)*, the average crossing speed for a young pedestrian was 1.51 m/s and they found an average crossing speed of 1.25 m/s for older pedestrians through a field survey conducted in Florida. Chandra and Bharti *(26)* also found an average pedestrian crossing speed of 1.5 m/s in a unidirectional crossing facility in India. For our project, the range of pedestrian crossing speed was selected from 0.5 – 2.5 m/s with an average value of 1.5 m/s. Time to collision (TTC) is an excellent indicator for pedestrian safety and length of active region depends on TTC. Jeong et al. *(27)* used a value of 2 s for TTC. For this simulation work, we used TTC values from 1.7 – 3 s for active region time. Regarding the vehicle speed, the maximum vehicle speed should be within a range of 25 – 35 mph or 11 – 15 m/s and cruising speed should be 12 mph or 5.4 m/s approximately *(28)*. The range of vehicle speed was selected from a range of 1 – 15 m/s in this project. The initial input parameters were selected based on existing studies and their values are provided in TABLE 12. Simulation results were generated based on selected combinations of input parameters mentioned above. Based on the data generated by the integrated simulation framework, qualitative and quantitative evaluations were conducted.

TABLE 12: Initial input parameters and their range of values

Parameters	Values	Distribution
Pedestrian initial speed	0.5 – 2.5 m/s	Normal
Vehicle initial speed	1 – 15 m/s	Normal
Time of active region	1.7 – 3 s	Normal
Pedestrian type	1 (cautious), 2 (risk-taker), 3 (distracted)	N.A.
Sensor type	1, 2, 3	Uniform

3.4.2 QUALITATIVE EVALUATION

Three types of sensors were used for pedestrian detection, and they were classified based on the percentage of detection error. Three simulations were done where all initial input parameters were kept the same except sensor types to visualize the variances in pedestrian detection process by the ASB. The noise around the position of pedestrian was found higher for type 3 sensors. FIGURE 24 illustrates the noises around pedestrian position for three types of sensors.

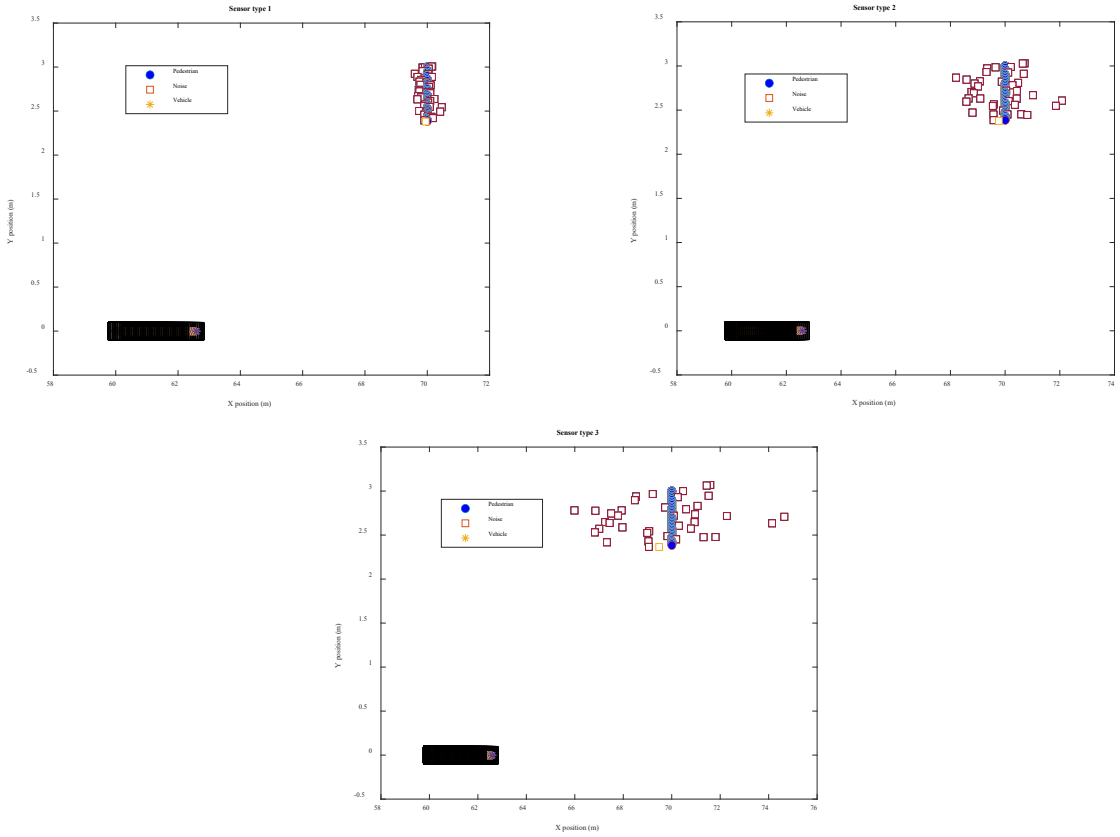

FIGURE 24: Detection error for different types of sensors

For comparing the crossing behavior for different types of pedestrians, another set of three simulations were conducted by changing the pedestrian types while keeping the other initial parameters as constants. Cautious pedestrian kept a maximum safe distance from the autonomous vehicle from starting of the simulation. On the contrary, distracted pedestrian came very close to the vehicle during crossing. Risk-taker pedestrian tried to cross the road from beginning of simulation but paused its movement if distance from the ASB decreased and the situation was unsafe for crossing. FIGURE 25 shows the variations of crossing behavior for different types of pedestrians.

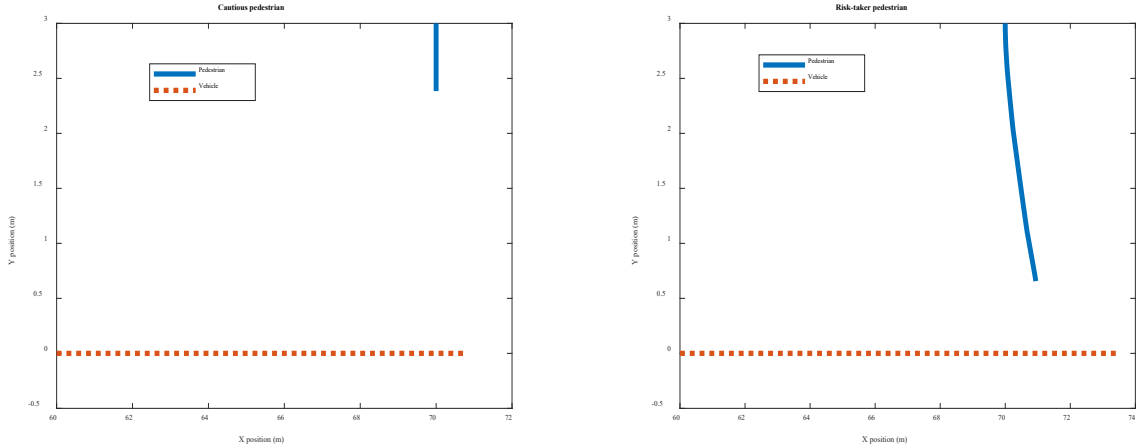

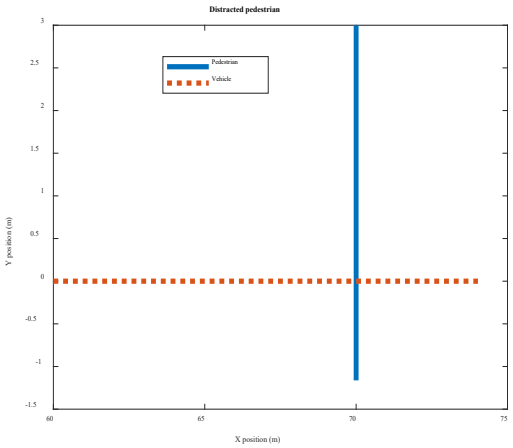

FIGURE 25: Crossing behavior of pedestrians at the crosswalk scenario

Another set of three simulations were conducted for evaluating the LSAV-VRU interaction pattern for the roundabout scenario. Only pedestrian type was changed while other input parameters were kept as a constant. The results were similar to the crosswalk scenario. Cautious pedestrian kept a certain distance from the beginning while risk-taker pedestrian came very close to the ASB and stopped for safety. Distracted pedestrian crossed the road in an unsafe manner. FIGURE 26 shows the crossing pattern of different types of pedestrians at the roundabout scenario.

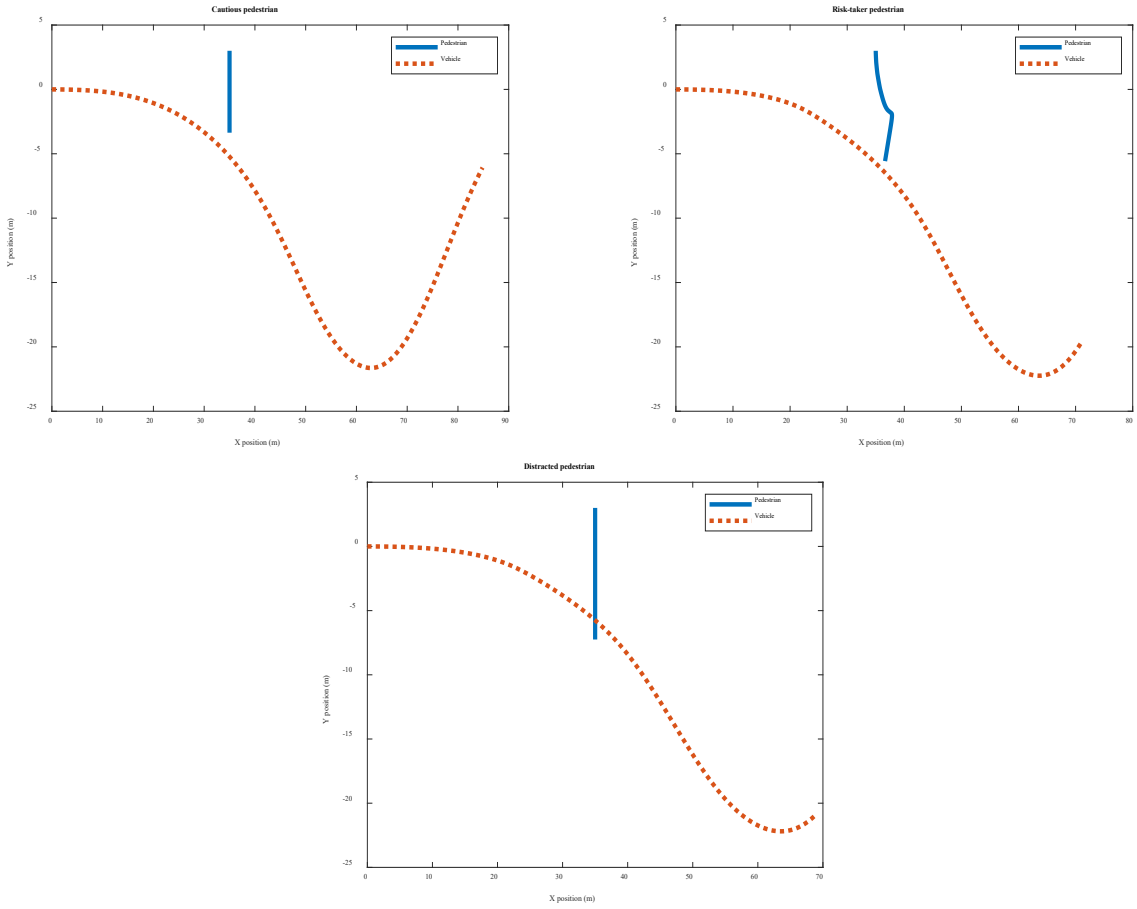

FIGURE 26: Crossing behavior of pedestrians at the roundabout scenario

From the qualitative evaluation, variations in crossing behavior were found for different types of pedestrians. Both cautious and risk-taker pedestrians avoided collision with the ASB by letting the vehicle pass before them. The vehicle also changed its speed accordingly when the pedestrian came very close to it. A successful negotiation was developed between road agents without compromising the traffic safety.

3.4.3 QUANTITATIVE EVALUATION

For the quantitative evaluation of simulation platform, a series of simulations were conducted for analyzing the variations in pedestrian/vehicle speed, AV's acceleration/deceleration to avoid colliding with the pedestrian, minimum safe distance between road agents, etc. All simulations were done with pedestrian initial speed 2 m/s, vehicle speed 7.5 m/s, risk-taker pedestrian type, type 2 sensor and active region time 2.2 s respectively. After generating the results of these simulations, the values were plotted for further analysis and discussions.

A contour plot was generated for demonstrating the change in speed of both pedestrian and vehicle during navigation for the crosswalk scenario. The initial speed of vehicle was set at 7.5 m/s at the beginning of simulation. As time of simulation progressed, the vehicle velocity decreased after detecting the approaching pedestrian. After crossing the conflict zone, the speed of vehicle increased again. For example, the minimum value of vehicle speed decreased to 1.21 m/s during interaction with cautious pedestrian and then increased again after passing the conflict zone. For risk-taker and distracted pedestrian, the minimum speed of vehicle were 2.37 m/s and 2.62 m/s respectively. Pedestrian speed for all cases decreased in a similar fashion during the interaction and increased again to reach to the destination point. FIGURE 27 shows the contour plot of speed change during interaction between ASB and cautious pedestrian at the crosswalk scenario as the simulation progressed.

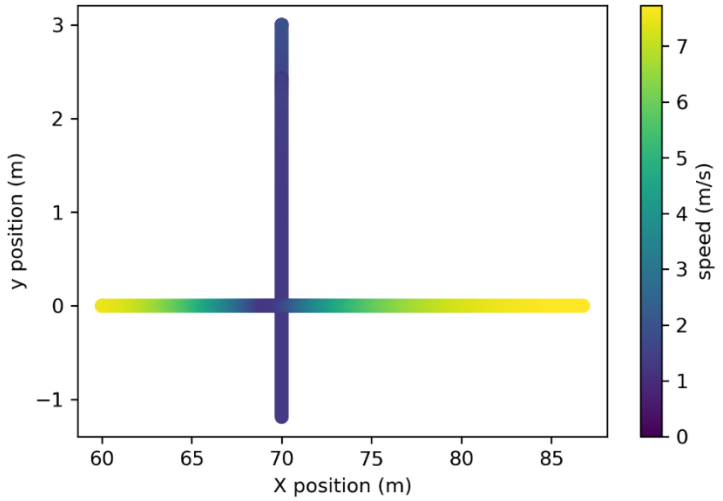

FIGURE 27: Trajectories of a cautious pedestrian and vehicle along with the contour plot of speed

Another simulation plot was generated for visualizing the control module of ASB during interaction with VRU. Due to the nature of the cautious pedestrian, it maintained a safe distance from beginning and the vehicle decelerated up to time of simulation, t = 1s and then it accelerated. On the other hand, the interaction time between ASB and remaining two pedestrian types was longer as both risk-taker and distracted pedestrian came closer to the vehicle than the cautious pedestrian. As a result, the vehicle decelerated up to 1.5 s of simulation and then it started

accelerating for navigation. FIGURE 28 illustrates the vehicle's control pattern during interaction with the cautious pedestrian at different timestep of the simulation process.

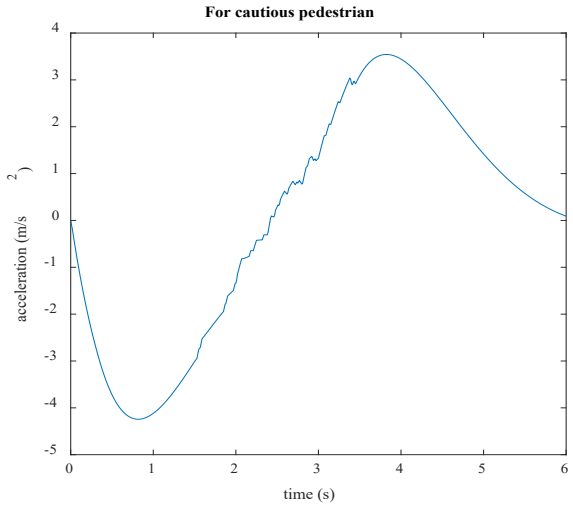

FIGURE 28: Vehicle's acceleration and deceleration during interaction with VRU

Minimum safe distance values that were accepted by different types of pedestrians during the interaction for both crosswalk and roundabout scenarios were extracted for comparison. The average value of these minimum distance along with their standard deviation (SD) values for both scenarios are provided in TABLE 13. The histogram plots of minimum distance values of the crosswalk scenario were plotted in FIGURE 29.

TABLE 13: Minimum accepted safe distance by pedestrians

Pedestrian type	Crosswalk scenario		Roundabout scenario	
	Mean (m)	SD (m)	Mean (m)	SD (m)
Cautious	2.72	0.42	6.42	1.62
Risk-taker	1.77	0.72	3.11	1.43
Distracted	1.48	0.70	2.12	1.11

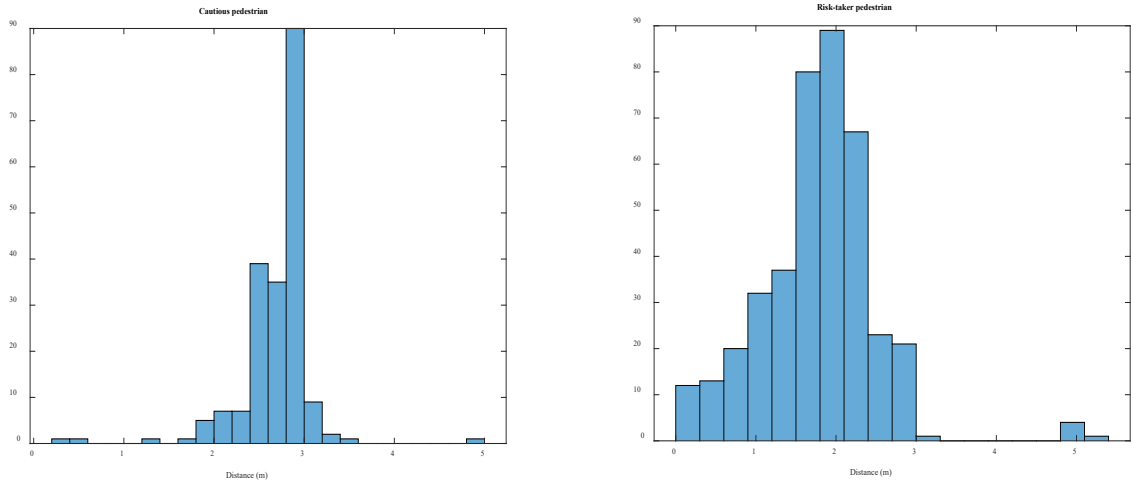

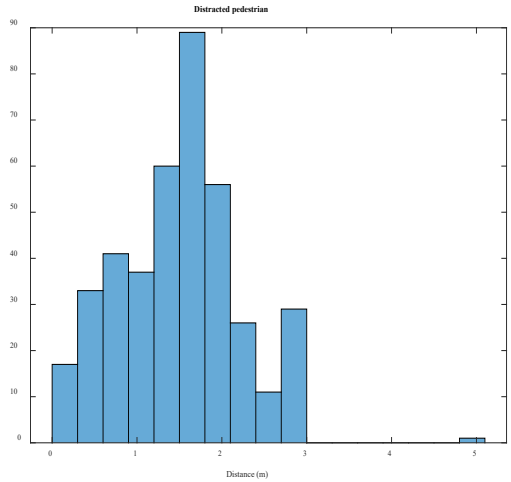

FIGURE 29: Histogram of minimum safe distance accepted by different types of pedestrians for the crosswalk scenario

From TABLE 13, it was found that the minimum safe distance accepted by cautious pedestrian for both scenarios was higher than other pedestrians and the average values were 2.72 m and 6.42 m for crosswalk and roundabout scenarios respectively. Due to the nature of the distracted pedestrian, unsafe road crossing occurred, and the mean accepted distance for crosswalk and roundabout scenarios were 1.48 m and 2.12 m respectively. The mean accepted distance for the risk-taker pedestrian were 1.77 m and 3.11 m for two scenarios respectively.

3.4.4 DISCUSSIONS OF ASB-VRU INTERACTION FRAMEWORK RESULTS

An integrated simulation platform was developed by combining pedestrian motion model, vehicle model, planning and control module of vehicle to assess the safety of interaction between VRU and ASB. The results generated from the simulation framework are as follows:

a) *Pedestrian's crossing behavior based on risk acceptance:* Three types of pedestrians were used in the simulation platform: cautious, risk-taker and distracted and their crossing behavior was found to be different as shown in FIGURE 25. In this figure, all trajectories were extracted at time of simulation, t = 3 s. Due to the nature of the cautious pedestrian, it kept a safe distance of 2.96 m from the vehicle. At the same timestep, risk-taker pedestrian came closer to the vehicle at a distance of 0.73 m and then stopped to let the vehicle pass for ensuring traffic safety. On the contrary, the distracted pedestrian already crossed the road at that timestep which led to a dangerous crossing. In reality, a distracted pedestrian can come very close to the navigation path of ASB and cause a risky situation that can hamper traffic safety. Vehicle algorithms should be developed to handle these high-risk scenarios for ensuring a safe interaction with pedestrians.

b) *Adaption of speed during navigation:* A safe negotiation between pedestrians and ASB is a must at crosswalks for maintaining traffic safety. Before crossing the road, a pedestrian evaluates the scenario by judging the relative position of vehicles and decides whether it is safe or not to cross. This is a continuous process that happens in the subconscious mind of the pedestrian, and it adapts speed either by increasing or decreasing to cross the road safely. The simulation platform was able to regenerate this phenomenon. For example, the speed of the vehicle was 7.5 m/s at the beginning of simulation as shown in FIGURE 27. Before reaching the conflict point, vehicle

speed decreased to 2.37 m/s when pedestrian was close and increased again after passing conflict zone. The risk-taker pedestrian also started with a speed of 2 m/s at beginning and decreased its speed to 1.48 m/s before coming to a complete stop for a safe interaction with the vehicle.

c) *Minimum safe distance during interaction:* Minimum safe distance accepted by different types of pedestrians can be useful for AV algorithms because the vehicle can apply appropriate strategies so that this minimum distance is always kept. From FIGURE 29, the distracted pedestrian came very close to AV and the mean safe distance was 1.48m. In the simulation platform, the ASB successfully maintained a safe distance to avoid collision with pedestrian. The minimum accepted distance values shown in TABLE 13 is also useful for determining high-risk crossing scenarios and they were used to simulate dangerous road crossing scenarios in the following section.

3.5 FINITE ELEMENT SIMULATION

3.5.1 INTRODUCTION

In the LSAV-VRU interaction simulation earlier, collision with the pedestrian was not allowed and the vehicle always decelerated/stopped to avoid hitting the crossing pedestrian. A finite element (FE) simulation was conducted in LS-DYNA software to simulate another scenario when the vehicle cannot stop before the pedestrian and crash cannot be avoided. There can be several reasons for collision such as ASB's sensor failure, or arrival of pedestrian at the last moment so brakes cannot be applied. The FE simulation was conducted to assess the pedestrian risk injury in case of unavoidable traffic accidents.

The most injured body parts in pedestrian collision with vehicles are head and lower extremities. Head injuries can cause fatal injuries to human body followed by chest injuries *(29)*. Many researchers studied the dynamic response of pedestrians during vehicle collisions *(30)*. Two types of simulation approaches were used in these vehicle-pedestrian impact simulations: multi-body approach or FE simulation approach *(31)*. For multi-body pedestrian impact simulation, MADYMO pedestrian human body model has been used which was validated by using impact testing on cadavers *(32).* Peng et al. *(33)* measured both pedestrian and bicyclist head injury response during a collision with a passenger car by using MADYMO model in PC Crash software. In another study by Han et al. *(29)*, effect of vehicle's velocity and frontal shape on pedestrian injury risk was evaluated by using FE model.

For this project, a FE model of Anthropomorphic Test Dummy (ATD) was used to measure risk injury in head and chest region during impact with a vehicle model. The ATD was a rigid Hybrid III 50^{th} percentile male standing dummy model available in LS-DYNA *(34)*. FIGURE 30 illustrates the ATD model that was used in the FE simulation. The vehicle model was developed in LS-DYNA by using the vehicle configuration from OLLI self-driving bus *(35)*. The length, width and height of the bus is 3920 mm, 2050 mm, 2500 mm respectively. The weight of the bus is 2650 kg. FIGURE 31 shows the OLLI minibus and developed rigid body vehicle model.

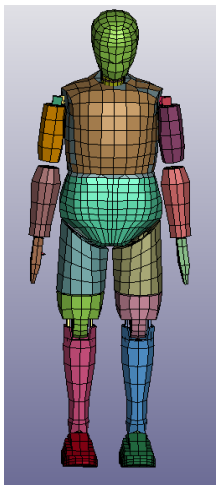

FIGURE 30: Hybrid III 50th percentile male standing dummy

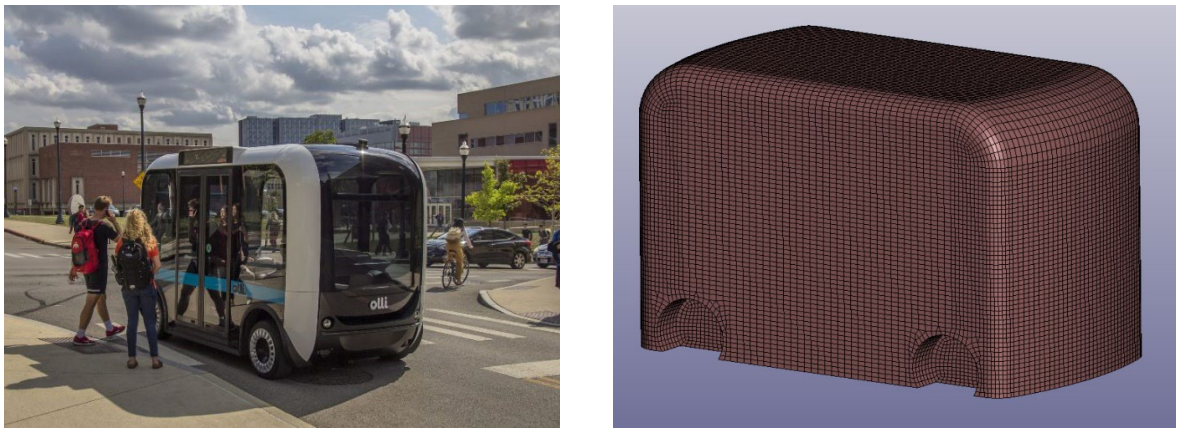

(a) (b)

FIGURE 31: (a) Low speed ASB (35)**; (b) rigid model of the vehicle developed in LS-DYNA**

In the finite element simulation, the rear part of the vehicle was kept as a rigid body, but the frontal part of the vehicle followed realistic stiffness corresponding to windshield, bumper, and metallic body parts. FIGURE 32 shows the vehicle model. This modification was necessary to produce accurate impact response.

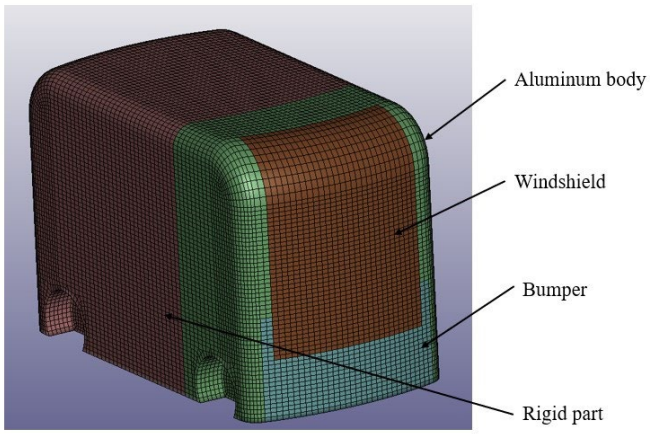

FIGURE 32: Modified FE vehicle model

Material properties of those body parts were validated by using the existing Toyota RAV4 (1997) FE vehicle model available in National Highway Traffic Safety Administration website *(36)*. First, the total mass of the SUV model was matched to the mass of OLLI minibus by adding extra mass to the RAV4 model. A simulation was conducted where the SUV hit a rigid wall. After the impact, total amount of load applied on the rigid wall and displacement in the bumper of the SUV were measured. A metal plate was then added behind the bumper of the FE vehicle model and another simulation was conducted where the FE model hit a rigid wall. Total load applied on the rigid wall and displacement in the metal plate were obtained and compared with the load-displacement values of the Toyota RAV4 model. FIGURE 33 illustrates the approach used for the validation of the FE vehicle model. By using several trials, the impact that will be applied to the pedestrian from the FE vehicle model was validated. TABLE 14 shows the maximum displacement and load applied on the rigid wall for both RAV4 and FE vehicle models.

TABLE 14: Maximum load applied on the rigid wall and displacement values in the bumper

	Displacement (mm)	**Maximum load (KN)**
Toyota RAV4	52	679
FE vehicle model	54.7	742

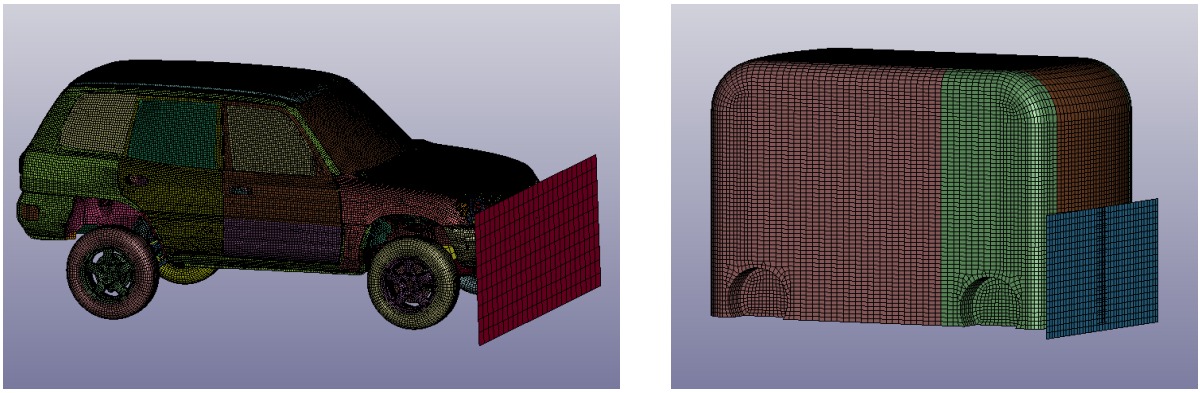

Toyota RAV4 hits the rigid wall FE model hits the rigid wall

FIGURE 33: Validation of the frontal part of FE vehicle model

3.5.2 PEDESTRIAN RISK INJURY CRITERIA

Injury criteria is developed based on the kinematic response of crash test dummies which can represent severity of risk of injury or to life of a human being. Most of these values have been obtained by using human cadaver. The mechanical behavior is also proportional to the amount of force or motion applied to the structure *(37)*. Measurable parameters such as force, velocity, acceleration, displacement, stress etc. have been obtained along with injury consequences to the test human subject body. A relationship between forces/motions and injuries are developed by following different statistical approaches. From these results, different Injury Assessment Reference Values (IARV) are developed for different body parts.

IARV values follows biomechanics and deals with movement of different body parts when forces are acting on a living organism. Biomechanics can be used to develop safety measures in vehicles and prevent injury to human body *(38)*. Gravity of injury is found to be influenced by the acceleration in different body parts produced by the crash

(39). As a result, risk injury criteria values have been developed based on the acceleration in human body parts. These values can also be used to determine severity of crash by utilizing different types of injury scales such as Abbreviated Injury Scale (AIS) etc. *(40)*. For this project, head injury criteria (HIC) and 3-ms chest acceleration criteria have been selected to assess pedestrian risk injury during crashes.

HEAD INJURY CRITERIA

Head injury criteria evaluates the injury risk caused to head during collision. It is based on the acceleration values in head and follows Eq. 9.

$$\text{HIC} = \left[\frac{1}{t_2 - t_1} \int_{t_1}^{t_2} a dt\right]^{2.5} (t_2 - t_1) \tag{9}$$

Where a = head resultant acceleration and $(t_2 - t_1)$ is time interval. t_1 is the initial and t_2 is the final instance of a time interval during which HIC value reaches to maximum. NHTSA limits the time interval for calculating HIC to 36 ms and maximum value of HIC to 1000 for the 50th percentile male *(37)*. The HIC values are linked to an Abbreviated Injury Scale (AIS) to describe the severity of injury in head are provided in TABLE 15. NHTSA proposed the AIS values of head injury ranging from 1 to 6. Bellavia et al. *(42)* generated fatality percentages for different ranges of HIC values where fatality percentage is obtained for AIS. The plot is shown in FIGURE 34.

TABLE 15: Head Injury on AIS scale *(41)*

AIS code	Description
1	Skin and scalp: abrasions, superficial lacerations. Face: fracture of the nose.
2	Leather: more abrasions. Simple or decomposed fractures to the face, open fractures or displacements of the jaw, fractures of the jaw
3	Different fractures, total loss of scalp, bruises to the cerebellum.
4	Complex facial fractures, exposure or loss of brain tissue, small epidural or subdural hematoma
5	Greater penetration of brain injuries, damage and hematoma to the trunk, epidural or subdural compression, axonal damage spread
6	Mass destruction of both the skull and the brain

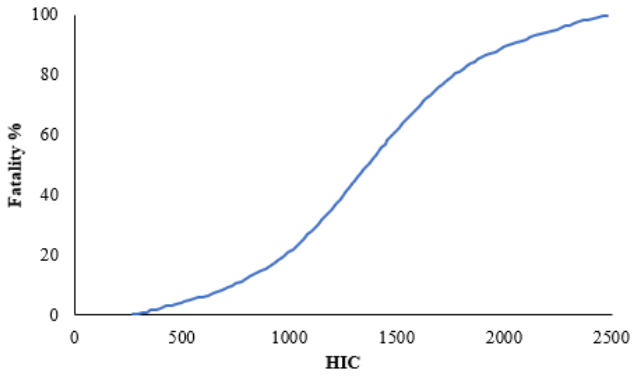

FIGURE 34: Percentage of fatality vs HIC plot

CHEST ACCELERATION CRITERIA

The chest injury criteria is based on Wayne State Tolerance Curve *(43)*. It is used in both US and European regulations for injury criteria. According to this injury criteria; both center of gravity of chest and head do not endure a higher

acceleration than 60g and 80g respectively for a longer time than 3 ms *(40)*. Probability of AIS 4+ chest injury is determined by Eq. (10).

$$\text{Probability (AIS 4 +)} = \frac{1}{1+\exp(4.3425-0.0630g_t)} \quad (10)$$

Here, g_t = maximum of the absolute value of the lateral acceleration in 'g' and the curve is shown in FIGURE 35.

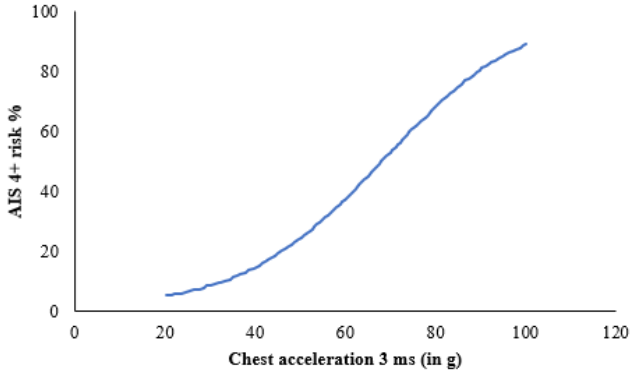

FIGURE 35: AIS 4+ risk % vs chest acceleration plot

3.5.3 FE SIMULATION PARAMETERS

From the LSAV-VRU interaction framework, it was found that traffic interaction occurred between road agents when vehicle speed was not too high or too low. For simulation scenario where vehicle speed was lower (1-4 m/s), pedestrian already crossed the road before the vehicle arrived. On the contrary, the vehicle passed quickly before it interacted with the pedestrian if initial vehicle speed was high (greater than 10 m/s). In this research, vehicle speed was selected from 5-10 m/s with an increment of 1 m/s. According to Kong and Yang *(44)*, the fatality risk percentage was found 8-34% for vehicle impact velocity of 50 km/h and 2-7% for vehicle impact velocity of 30 km/h in China based on accident datasets. In this simulation, two types of pedestrian impact were tested: frontal impact and side impact. For frontal impact, pedestrian face was positioned towards the vehicle and for side impact, pedestrian face was set towards the road before collision. These different types of vehicle impacts are illustrated in FIGURE 36. The output of the FE simulation was HIC and 3 ms chest acceleration injury criteria respectively obtained from LS-DYNA d3 plot files.

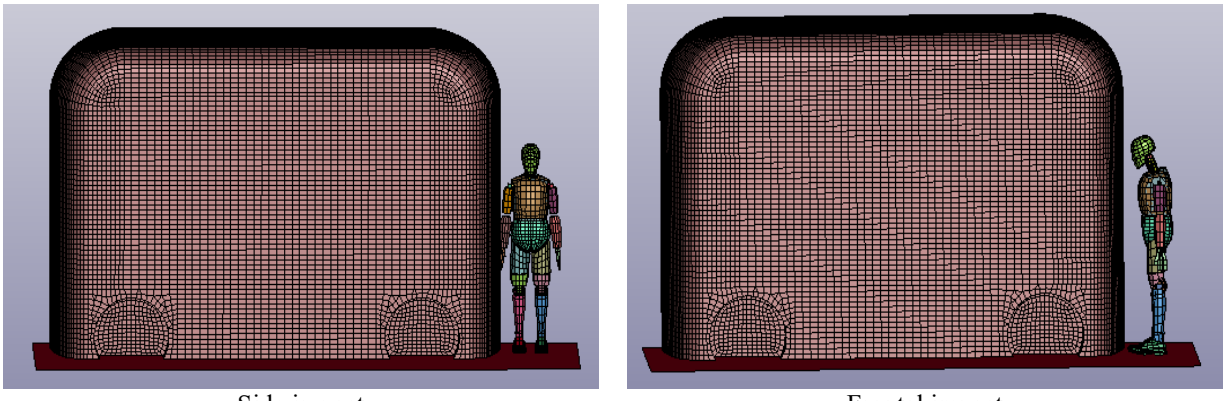

Side impact Frontal impact

FIGURE 36: Different types of vehicle impact

Pedestrian kinematics at different timesteps have been obtained from LS-DYNA output to visualize the difference between side impact and frontal impact scenarios. The initial impact velocity was fixed at a constant value

of 8 m/s for visualizing the pedestrian kinematics. During the side impact scenario, pedestrian's lower extremities and chest contacted the vehicle windshield at 20 ms of simulation. Pedestrian's head then touched the windshield after 40 ms of simulation time. Deformation was observed in the vehicle after hitting the pedestrian. At 55 ms of simulation, windshield along with bumper cover, metal body parts deformed in the opposite direction of vehicle motion as shown in FIGURE 37.

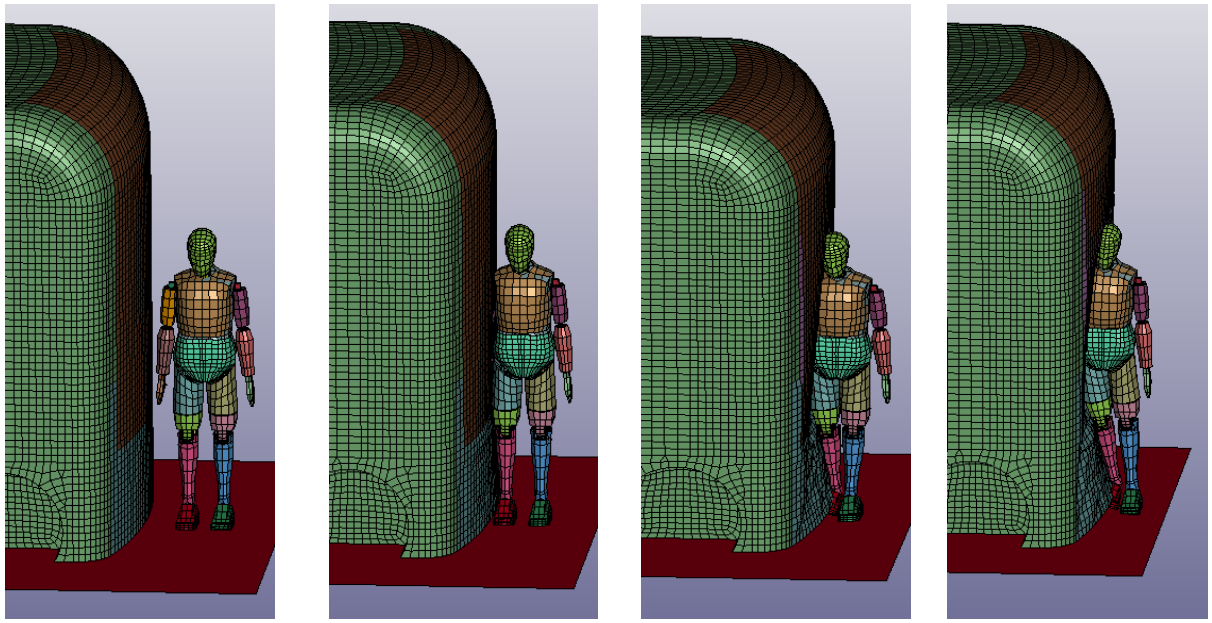

0 ms 20 ms 40 ms 55 ms

FIGURE 37: Pedestrian kinematics during the side impact scenario

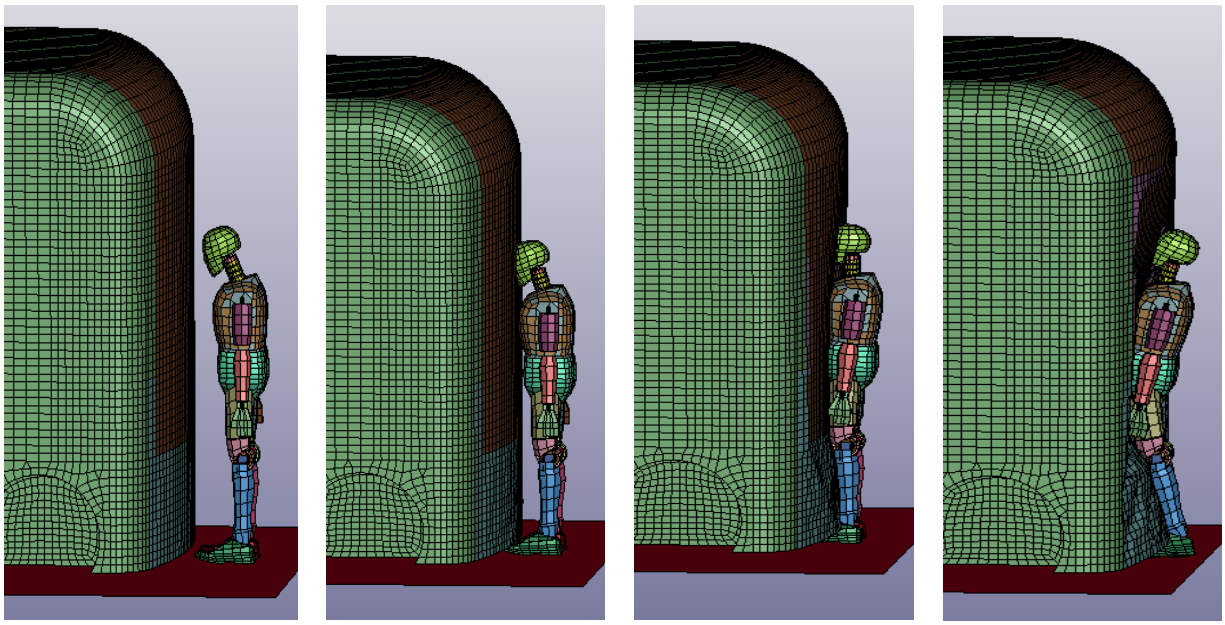

0 ms 15 ms 35 ms 60 ms

FIGURE 38: Pedestrian kinematics during the frontal impact scenario

In the front impact scenario, pedestrian's head contacted the windshield at 15 ms of simulation. At 35 ms, chest and pelvis portion of the pedestrian contacted the vehicle and rotation of pedestrian body was observed after 60 ms of simulation. Similar pattern of vehicle deformation during side impact was also found in the front impact scenario. FIGURE 38 illustrates the pedestrian kinematics during the frontal collision.

3.5.4 SIMULATION RESULTS

Total 24 simulations were done in LS-DYNA software for determining the pedestrian risk injury criteria. Initial speed of the vehicle was selected as 5, 6, 7, 8, 9 and 10 m/s and two types of impact (side and frontal) were considered FIGURE 39 illustrates the vehicle speed vs HIC plot. HIC value increased when vehicle speed increased. HIC values were found to be higher for frontal impact than side impact as pedestrian head received vehicle impact earlier in frontal impact scenario. The HIC values obtained in the simulation followed the pattern found in the study of Mizuno and Kajzer *(45)*. This paper obtained the HIC values for pedestrian collision with a minivan where pedestrian's head contacted the windshield and the range of HIC values in this type of collision was 0-500. Another study done by Han et al. *(46)* simulated pedestrian head injury with a one box type vehicle (Honda ACTY) and the HIC values was 338 with vehicle initial speed of 40 km/h or 11.11 m/s.

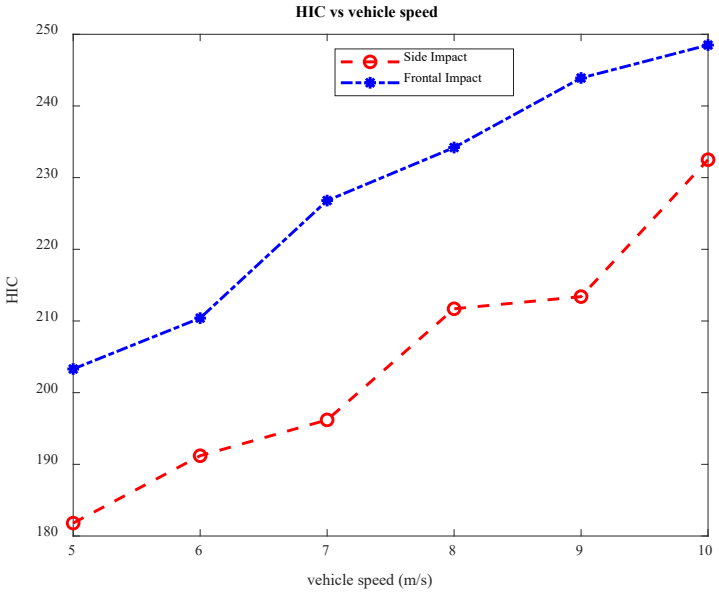

FIGURE 39: HIC vs vehicle impact speed plot

FIGURE 40 illustrates the chest acceleration vs vehicle speed plot. Chest acceleration values were higher for the frontal impact simulation. In both scenarios, chest acceleration values increased when vehicle speed increased. The values of chest acceleration ranged from 10g – 15g for side impact scenarios and maximum values for frontal impact was 36g. Han et al. *(46)* also found 50g chest acceleration in their study with one box vehicle (Honda ACTY) - pedestrian collision.

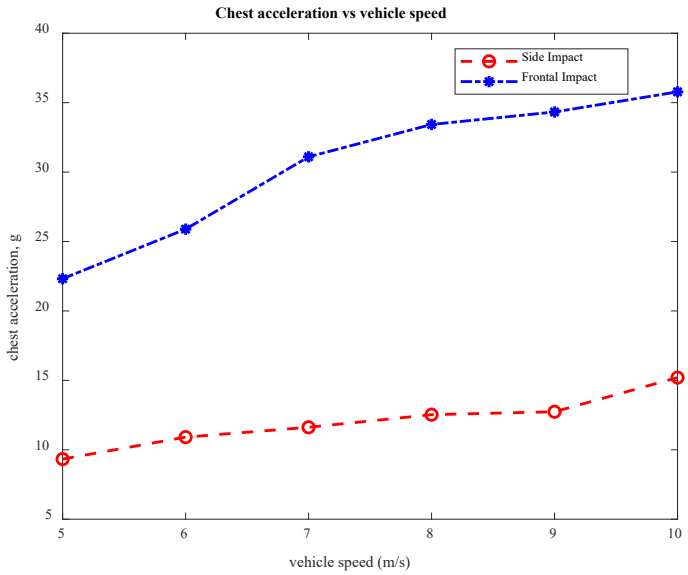

FIGURE 40: Chest acceleration vs vehicle speed plot of modified vehicle model

Using the simulation results and FIGURE 34, the percentage of fatality was obtained for both side and frontal impact scenarios, for the vehicle speeds between 5 and 10 m/s. The fatality percentage for the side impact was negligible. The fatality percentage due to head injury was low (less than 5%) for all simulations. Similarly, check risk injury risk was obtained using the simulation results and FIGURE 35. The chest injury risk was relatively low (close to 10%). From the finite element simulation results, it can be seen that both head injury criteria (HIC) and chest acceleration values increased when vehicle impact speed increased.

4 EVALUATION OF TRANSIT PROPERTIES

4.1 OPERATIONAL DESIGN DOMAIN (ODD)

The operational design domain (ODD) describes the specific operational conditions under which the automated driving system (ADS) can safely function *(47)*. The ODD includes but is not limited to the following information of ADS' operational characteristics: roadway types, speed range, geographic area, environmental conditions such as weather conditions, and illumination. According to the latest report published by (1), the low-speed automated vehicles (LSAVs) that are operating in public in the US, vary in speed, level of automation, size, compliance with ADA. Therefore, depending on the level of automation and the manufacturers, different ODD has been defined for these vehicles based on the operational conditions and manufacturers. LSAVs have been implemented and operated by different public and private entities for the following purposes:

- *Service models:* provide mobility services in fixed routes, circulators, shuttles, first/last miles, and paratransit or combination of them.
- *Trip purposes:* They are mostly implemented by organizations that are not public transportation sectors, and provide services for health care, employment, entertainment, senior social services, etc.

The key aspects of the ODD for LSAVs are operational speed, weather, traffic condition, roadway characteristics, and roadway conditions. There might be some other factors such as time-of-day restrictions and certain traffic conditions. For example, in a pilot test conducted by *(48)* using the electric Olli shuttle bus, they restricted the operation to daytime because the lighting system can increase the battery usage.

The main factor that determines the complexity of the ODD is the level of interaction with other road users and more specifically pedestrians. Most LSAVs implement a very conservative way to interact with VRUs using the right-of-way principle. This will minimize the likelihood of having unexpected edge case scenarios but has its downsides such as a decrease the operational speed, potential traffic congestions, and risk of rear-end crash. Additionally, studies have shown that pedestrians may take advantage of LSAVs due to their predictable behavior which can cause the 'freezing robot problem.' Therefore, the LSAV must have a plan to overcome all of those issues and the developers must consider these aspects in their decision-making algorithms.

The related scenarios for LSAV-VRU interactions can be divided into four categories. See FIGURE 41. Area 1 represents the known-safe scenarios. These are the scenarios that the vehicle can safely control and handle and fall well within the ODD. The vehicle systems were validated and verified against these scenarios in terms of both functional and operational safety. Area 2 shows the known-unsafe situations. These are the scenarios that are out of the ODD of the LSAV and the designers know that the vehicle cannot operate safely in those situations. These scenarios must be identified and the countermeasures and proper mitigation strategies such as system corrections must be taken to reduce the overall risk of the system. Once the vehicle systems were improved and demonstrated that they can safely operate in those scenarios they were classified under area 1.

Area 3 refers to the unknown-unsafe scenarios. These scenarios are unknown and also unsafe that the vehicle cannot perform safely. These scenarios can be discovered using a combination of different methods such as on-road and track testing and simulations. Once these scenarios are identified, they are reclassified under area 2. Area 4 shows the unknown scenarios, but they are safe and they are not a matter of concern for developers. The black arrows in FIGURE 41 show the direction that must be taken to define and expand the ODD of the safe operation of LSAVs the goal is to minimize the area 3.

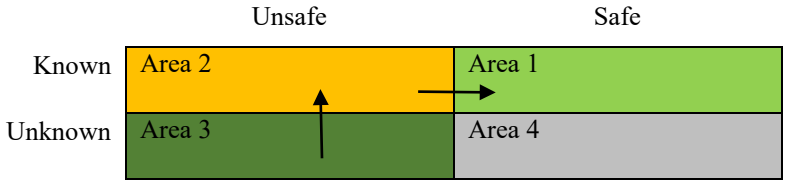

FIGURE 41: Visualization of different scenarios for the safety of LSAV

While automated public transportation systems have a potential to increase safety in various domains, they also add complexity especially in how these systems could and should interact with other road users. This requires new risk assessment and safety verification methods to ensure that autonomous systems meet or exceed the reliability of human. However, it is not straightforward due to the complexities of pedestrian behaviors, and computer codes that are embedded in automated vehicle. Therefore, knowledge regarding the overall system components, their interactions, and critical applications can provide effective tools to evaluate the risk and safety of this new technology.

The system theoretic process analysis (STPA) was used to define each component and its interactions. This approach is based on system theory that provides the mathematical foundation for STPA. In STPA, safety is treated as a dynamic control problem rather than a failure prevention problem. This is very effective in the safety analysis of complex systems *(49)*. FIGURE 42 shows the control loop structure of the system. Four steps must be defined in order to conduct the hazard analysis: 1) Defining the losses, system potential system-level hazards and system-level constraints; 2) Modeling the control structure based on all the components of a system; 3) Identifying the unsafe control actions (UCAs); 4) Identifying the loss scenarios and contextual characteristics.

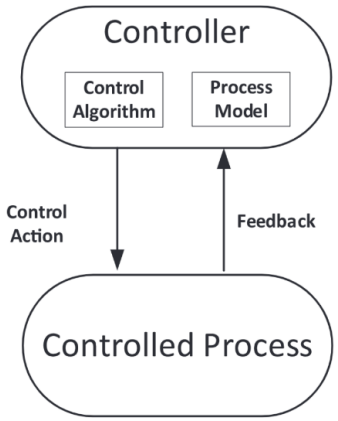

FIGURE 42: The concept of STPA control loop

To provide a better understanding of transit properties and evaluate the safety, a system approach framework for LSAV-VRU safety analysis has been developed (see FIGURE 43). The STPA diagram contains seven blocks that are connected based on the control system. The components related to the vehicle are perception, human-machine interface, prediction, and planning system, control, and vehicle body. The environment block has all the static and dynamic elements regarding infrastructure, road, dynamic and static objects on the road, traffic signs, and rules. Finally, the human safety operator can intervene with the driver tasks if needed. For some cases this is replaced by the tele-operation that provides required inputs for the vehicle to have a safe maneuver. The blue arrow from the human-machine interface to the environment is considered for any communication system that a vehicle can have with pedestrians (considered dynamic objects).

Although the purpose of an automated driving system is to remove the human from the loop, for the safety purpose, at this stage, most of the automated shuttle buses operate with a human safety operator or remote operator from the monitoring center. Because in the event of any unexpected behavior which could potentially trigger risk for passengers and other road users, the human safety operator intervenes and take the control of the automated vehicle. For the cases that the safety driver performs the monitoring tasks, he/she can interact with environment and vehicle as shown by two black arrows in FIGURE 43. The human-machine interface must provide proper, straightforward and effective instruction to driver for situations that require his/her input. Due to the nature of public transportation services, usually, the driver does not only perform the driving tasks, but he also assists disabled passengers and controlling the doors. So, it is a fair assumption that the driver cannot be completely removed from the autonomous transit bus fleet for the foreseeable future.

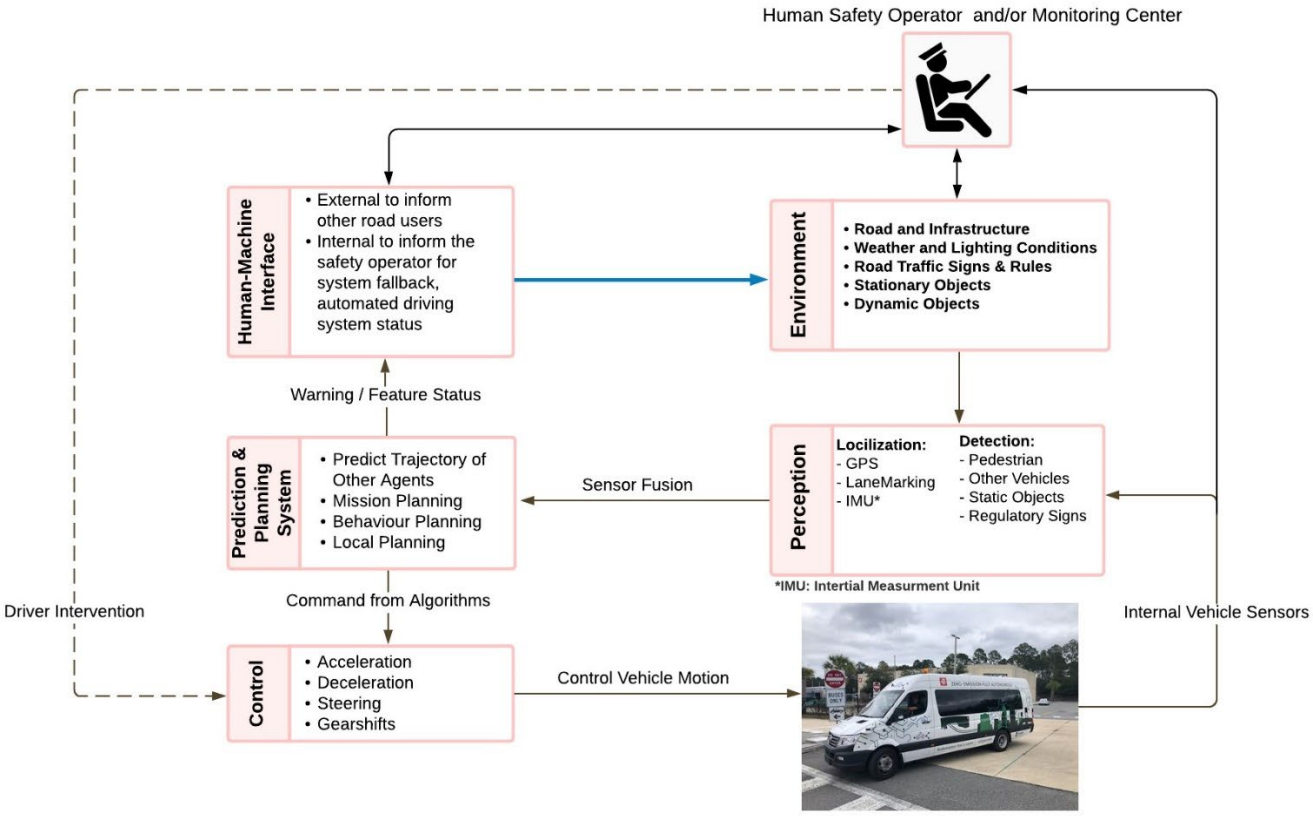

FIGURE 43: Automated shuttle bus block diagram for safety analysis based on STPA

This framework was used for qualitative risk assessment regarding the pedestrian and automated shuttle bus that resulted from any unsafe actions that might happen either from vehicles or pedestrians. FIGURE 43 shows the close-loop control model that was developed for the ADAS systems for transit buses. This model has seven blocks that are connected based on their relationship. The blocks are as follows:

- *Safety Driver (controller):* The driver can have two actions brake, accelerate or steering at emergency situation
- *Human-machine interface:* It is a panel for communication and controlling the autonomous mode
- *Perception &Planning system (controller):* Contain the decision-making algorithms based on mathematical logic
- *Perception:* Contains all sensor stack components to obtain all the information required for localization and object detections
- *Control module (actuator):* Convert the input from safety driver and Planning module systems to actions in the vehicle
- *Vehicle (controlled process)*
- *Environment (input to the system):* Contain all other traffic elements on the road

To ensure that the system shown in FIGURE 43 can address the prevention or mitigation mechanisms for any unsafe interaction with vulnerable road users, the attention must be focused on how that system fails or misbehave rather than how it works *(50)*. One way to address that is by following these steps: 1) Identify the hazards 2) Building scenarios to identify those hazards; 3) Define certain criteria for test performance measurements (pass or fail). Based

on the STPA method, a hazard occurs when the system controller (safety driver, planning module) issues an unsafe control action or fails to issue a control action needed to maintain a safe operation of vehicle. Also, each control action can be analyzed considering following general cases:

- Not provided when needed to maintain a safety
- Provided when control action is not needed and causes a lose
- Provided but the duration is too short or too long
- Provided but starting time is too soon or too late
- Provided but the intensity is incorrect (too much or too little)

In the context of this project, we need to first define the loss regarding the LSAV- VRU interactions. Then we list all of the control actions that each controller (in our case driver safety and planning module) can issue. In our system, we have two controllers: the prediction & planning module and safety drivers. The actions that they can take are summarized into accelerating, braking, steering, and communicating. The communication can happen to inform the pedestrian, driver, tele-operation center, or emergency centers. Then for each control action a set of contextual information (road and environment, pedestrian characteristics, etc.) must be defined. We used the field transit crash data regarding pedestrian fatality to extract the contextual information and building the scenario. For example, a safety driver provides a brake too late when the LSAV did not recognized the obscured crossing pedestrian. In this unsafe control action, the driver is a controller, the control action is braking, and the unsafe control action is too late. The contextual information for this scenario is only the presence of pedestrian that is obscured. However, further operational situation can be provided to better understand the scenario details. In the following subsection, we tried to extract further contextual information for high-risk scenarios using field crash data analysis.

4.2 FIELD CRASH DATA ANALYSIS

Researchers and developers of AVs *(51)* and *(52)* have suggested using real-world crash data to identify the safety case scenarios. Information about the contextual elements of crashes are locations, crash severity, crash types, time of the day, lighting conditions, etc. The Federal Transit Administration (FTA) provided the detailed transit bus crash data from 2014-2020. This data contains several aspects of crashes such as the type of the bus, manufacturer, the crash location characteristics, the number of injured passengers, and fatality rate. Analyzing these data can provide a better understanding of the high-risk crashes regarding transit buses. TABLE 16 shows the crash data based on the type of crash that transit buses were involved. For example, these crashes occurred between the bus and other motor vehicles, or vulnerable road users (VRUs), or other transit buses, or fixed objects. The highest fatality rate was among the crashes between the bus and VRUs. In this database, the VRUs include both pedestrians and cyclists. However, in this project, we only consider the crash with pedestrians.

TABLE 16: Summary of transit bus crashes that occurred between 2014-2020

Crash between Transit Bus and	Fatalities	Total Number of Crashes	Fatality Rate (%)
Motor Vehicle	343	35213	1.0
Vulnerable Road Users	**676**	**5489**	**12.3**

Transit Bus	4	349	1.1
Fix Objects	5	1255	0.4

Further analysis of crash data revealed that the highest pedestrian fatal crashes (29% and 23% of total fatal crashes) occurred at revenue facilities and right-of-way roads as shown in FIGURE 44.

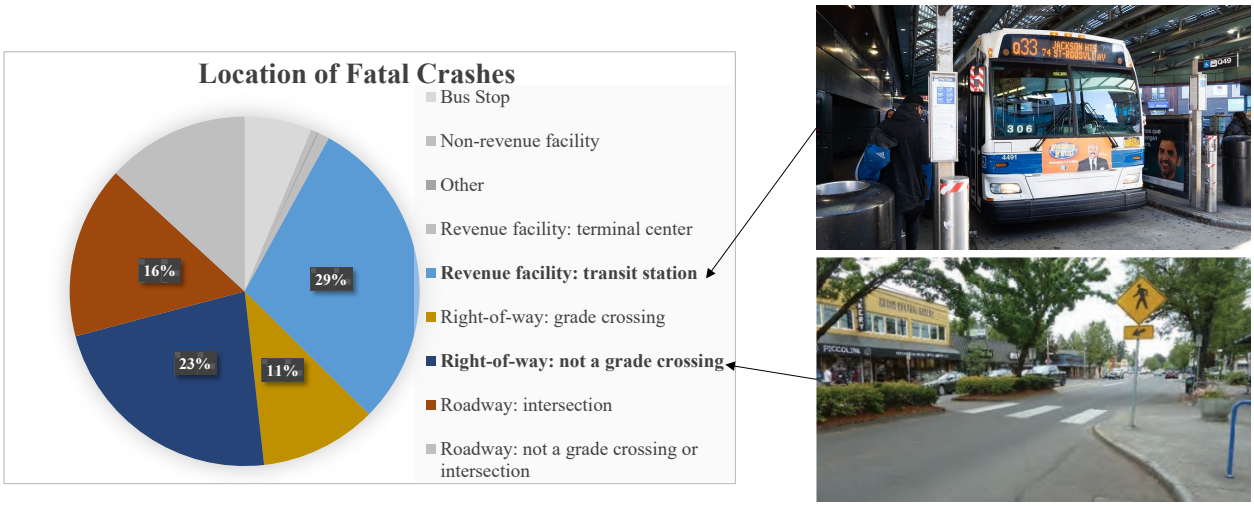

FIGURE 44: VRU fatal crashes based on the type of locations for transit buses *(53)*

As a result of these analyses, the two main scenarios were considered for the simulation of LSAV-VRU interactions. The first scenario is the crossing pedestrian that and the second scenario is the roundabout. FIGURE 14 and FIGURE 15 illustrate the scenarios that were considered for this project. A set of parameters regarding the vehicle, pedestrian, and road characteristics were considered to conduct the parametric study. The effects of vehicle parameters such as the speed range, detection capabilities, maximum and minimum deceleration were evaluated to identify the high-risk situations within these scenarios.

4.3 SCENARIO ANALYSIS

At this step, the test scenarios were defined based on the combined results of the STPA, field crash data analysis, simulations, and close-track tests. It is important to note that the risk assessment for LSAV-VRUs interaction assumes that the vehicle-system level is free of faults. This means that the motion control module can correctly translate the commands to maneuver for the vehicle (e.g., no brake or tire issue). The sensor stacks used for the perception must be functional within the ODD of the LSAV and errors must be within the acceptance range provided by manufacturers. Also, our focus in this analysis is on pedestrian safety issues without considering any cyber security concerns.

TABLE 17 shows the losses that were defined for this analysis. They were divided into two broad categories including physical and socioeconomic losses. The SEL1 and SEL2 were defined as losses that can have negative effects on customer satisfaction and market failure. These losses can lead to an incomplete trip or a very long trip which both can lead to loss of user acceptance in the public transportation sector. Furthermore, acceptance is defined as a combination of satisfaction, trustworthiness, and joyfulness factors when road users/passengers experience

interaction with LSAV. TABLE 18 shows different potential hazard along with related loss that has been defined in the scenario analysis.

TABLE 17: Loss definition

Physical Loss	Name	Socioeconomic Loss	Name
Life-threatening or Serious injury	PL1	Incomplete journey	SEL1
Collision with other objects	PL2	Time of journey being too long	SEL2

TABLE 18: Potential hazards definition

Potential Vehicle-Level hazards	Name	Related Loss
Not able to maintain a safe distance	H1	PL1, PL2
Lane or roadway departure	H2	PL1, PL2
Exceeds safe operational envelope	H3	PL1, PL2, SEL2
Expose harmful events to passengers (hard brake, door closes, etc.)	H4	PL1, PL2
Wrong communication message	H5	PL1, PL2, SEL1

TABLE 19 illustrates different scenarios that were taken under consideration along with related hazard and potential mitigation suggestions. The extreme scenarios where it is almost physically impossible to avoid collisions were also excluded. For example, if the LSAV driving at a maximum speed and suddenly a person comes out of his car and runs across the road in front of the LSAV (distance less than a meter), the crash likely occurs. Because even though the LSAV can detect the pedestrian with exact position and correctly predicts that he is going to cross the street, there is not enough time and space to bring the vehicle to a full stop. Of course, it would have been ideal to avoid these kinds of crashes, but due to the physical constraints that come with the current technology and mechanical characteristics of the vehicle, it is very challenging to design a system that can provide a safe maneuver to protect both pedestrians and passengers inside the vehicle.

TABLE 19: Scenarios, related hazard and potential mitigation

Scenarios	Potential Causal Factors	Related Hazard	Operational Situation	Mitigation
The vehicle may apply brake too early or too late when facing a pedestrian	Perception error	H1, H2, H5	Obstruction, deteriorated road surface, low quality of lane markers,	Perception capabilities and limitations must be fully identified and communicated with the operator and transit agencies
The vehicle may apply brake too hard or too slow	Perception error	H1, H2, H4, H5	Obstruction, deteriorated road surface, low quality of lane markers,	Perception capabilities and limitations must be fully identified and communicated with the operator and transit agencies
The vehicle may stop too far or too close to a pedestrian	Improper design for the Planning algorithm	H1, H2, H5	Rainy or icy road	The manufacturer or system designer must revise the algorithms and perform rigorous validation tests again

The vehicle may turn left or right sharply or very slow	Improper design for the prediction algorithm regarding the pedestrian future path	H1, H2, H5	Pedestrian walking alongside of the road,	The manufacturer or system designer must revise the algorithms and perform rigorous validation tests again
The vehicle does not keep a safe distance from the curb during embarkation/debarkation	The improper bus station and curb design or improper path planning	H1, H2, H4, H5	Different weather and road conditions	Effective communication with pedestrians who are waiting at the bus station, and ask for safety driver input
Vehicle approaching a pedestrian in an unsafe manner	Safety driver error	H1, H2, H3, H4	When approaching or leaving the crowded bus stations, approaching / existing a roundabout	Safety drivers should not be able to interfere with driving tasks in autonomous mode and only modify or correct the signals that go into the planning module
Vehicle freezes facing a group of pedestrians	Improper design for the Planning algorithm	H4, H5	Any weather types, shared roads with pedestrians	Effective communication with pedestrians who are waiting at the bus station, and ask for safety driver input

5 CHALLENGES, LIMITATIONS, AND LESSONS LEARNED

5.1 CHALLENGES OF AUTONOMOUS VEHICLES

Autonomous systems rely on probabilistic reasoning and models to recognize who, what, and where agents in road traffic scenarios are and what their next set of actions will be. This alone requires comprehensive and rigorous functional validation tests for autonomous systems to ensure that all of the tasks regarding recognition, prediction, and behavioral planning and their limitations are fully captured.

Although the field data analysis of transit buses can provide better contextual information about the pedestrian crash characteristics and where and when those crashes occurred, we cannot generalize those findings to all vehicles. This means that the LSAVs are expected to eliminate most of those crashes but might create new conflicts or unsafe situations for vulnerable road users, which is the main challenge that autonomous vehicle developers are facing today.

5.2 LIMITATIONS OF THIS STUDY

We reduced the complexity of our simulation analysis to utilize the available data. Two main limitations were as follows. First, the LSAV models have a different set of algorithms and sensor stacks *(4)* that cannot be represented by one simulation model. Second, due to the proprietary nature of data, the evaluation of pedestrian detection and the decision-making process followed models from the literature, which may be different from the tested LSAV.

We used the CITR dataset to compare and validate the pedestrian model's simulated trajectory. This dataset was collected from a controlled setup which can vary from real-world pedestrian crossing scenarios. We assumed a TTC threshold value for pedestrians. Although these values were extracted from the literature review; in the real world, this value can be varied based on individual characteristics such as age, gender, etc.

Single pedestrian was considered in the LSAV-VRU interaction framework. In reality LSAV has to deal with multiple pedestrians at the same time. Presence in a group can alter the road crossing behavior of a single individual

and LSAV should be able to interpret crossing intents. For example, the behavior of individual pedestrians is probably well understood but it is far from clear how ten pedestrians as a group would behave in the same traffic scenarios.

5.3 LESSONS LEARNED

1. The driver must have minimum interaction with the vehicle for a fully automated low-speed vehicle. This means that the vehicle must be able to operate safely in most traffic situations without requiring driver assistance. However, today's autonomous vehicle still needs driver actions, and for certain situations (e.g., roadside work, construction zones, etc.), the driver must provide proper input to the vehicle. Generally, a driver performs three tasks of recognition, judgment, and action to perform maneuvering. This requires a good understanding of vehicle status and all other scenarios parameters.
2. One of the key aspects of LSAV safe operation is to obtain sufficient knowledge regarding pedestrians and develop the data, skills, and methods for a systematic pedestrian safety analysis. This requires strong inter-jurisdictional collaboration amongst state DOTs and other transit agencies. There have been several active, planned, and completed projects in the US that will certainly provide valuable safety cases data *(1)*, especially regarding LSAV-VRUs interactions. These shared data can be used to obtain critical information about the safety performance of different LSAV types in different edge case scenarios and understand the important key aspects of their ODD. The transit agencies can play a critical role in collecting, sharing that information while keeping the proprietary information.
3. How road users feel safe when interacting with LSAV has a subjective nature. For example, how far away an LSAV should stop when a pedestrian is crossing in front of the vehicle highly depends on how closeness can affect the perception of comfort and safety for that specific road user. This is a challenging aspect that the developers of these technologies must address that considering social aspects.

6 FUTURE RESEARCH

Interaction between pedestrians and road traffic vehicles is one of the most complex problems in transportation safety. It has interdisciplinary characteristics — it has a connection with psychology, engineering, policy, and regulation. One key aspect of safe LSAV-VRUs interaction is to understand pedestrian behavior in different road traffic scenarios. The uncertainties of human characteristics such as reaction mechanisms *(54)* and path planning upon emergent traffic situations have not yet been understood. The public transportation agencies can collect this information using their proper tools and infrastructure. For example, video data from bus stations can provide valuable data in terms of how many people use the bus and how they behave around the bus stations. This allows them to have a more accurate assessment of LSAV-VRUs around these areas. Additionally, the new data-driven simulation models of pedestrian behavior can provide promising insights into how pedestrians make decisions in different traffic scenarios *(55)*. Another key aspect of LSAV-VRUs interaction is the demographic characteristics. Different types of demographic characteristics and their vulnerability in potential high-risk LSAV-VRU interactions can be focused on which can determine future acceptance rate of autonomous vehicle.

7 REFERENCES

1. Transportation PLAGEC for. Low-Speed Automated Vehicles (LSAVs) in Public Transportation. Low-Speed Automated Vehicles (LSAVs) in Public Transportation. National Academies Press; 2021.
2. Babb BA, Emery RE. October 2017. Vol. 55, Family Court Review. 2017.
3. Thorn E, Kimmel S, Chaka M. A Framework for Automated Driving System Testable Cases and Scenarios [Internet]. Dot Hs 812 623. 2018. Available from: https://www.nhtsa.gov/sites/nhtsa.dot.gov/files/documents/13882-automateddrivingsystems_092618_v1a_tag.pdf
4. Combs TS, Sandt LS, Clamann MP, McDonald NC. Automated Vehicles and Pedestrian Safety: Exploring the Promise and Limits of Pedestrian Detection. Am J Prev Med [Internet]. 2019;56(1):1–7. Available from: https://doi.org/10.1016/j.amepre.2018.06.024
5. Rodríguez P. Safety of Pedestrians and Cyclists when Interacting with Automated Vehicles: A Case Study of the WEpods. 2017;1–120. Available from: https://www.raddelft.nl/wp-content/uploads/2017/06/Paola-Rodriguez-Safety-of-Pedestrians-and-Cyclists-when-Interacting-with....pdf
6. Kong J, Pfeiffer M, Schildbach G, Borrelli F. Kinematic and dynamic vehicle models for autonomous driving control design. IEEE Intell Veh Symp Proc. 2015;2015-Augus(Iv):1094–9.
7. Wang C, Xie Y, Huang H, Liu P. A review of surrogate safety measures and their applications in connected and automated vehicles safety modeling. Accid Anal Prev [Internet]. 2021;157(June 2020):106157. Available from: https://doi.org/10.1016/j.aap.2021.106157
8. Rasouli A, Tsotsos JK. Autonomous vehicles that interact with pedestrians: A survey of theory and practice. IEEE Trans Intell Transp Syst. 2020;21(3):900–18.
9. Ridel DA, Deo N, Wolf D, Trivedi M. Understanding pedestrian-vehicle interactions with vehicle mounted vision: An LSTM model and empirical analysis. IEEE Intell Veh Symp Proc. 2019;2019-June:913–8.
10. Ismail K, Sayed T, Saunier N. Automated analysis of pedestrian-vehicle: Context for before-and-after studies. Transp Res Rec. 2010;(2198):52–64.
11. Rodríguez Palmeiro A, van der Kint S, Vissers L, Farah H, de Winter JCF, Hagenzieker M. Interaction between pedestrians and automated vehicles: A Wizard of Oz experiment. Transp Res Part F Traffic Psychol Behav. 2018;58:1005–20.
12. Lewandowski CM. Driverless Vehicles' Potential Influence on Cyclist and Pedestrian Facility Preferences. Vol. 1, Partial Fulfillment of the Requirements for the Degree Master of City and Regional. 2015.
13. Hagenzieker MP, van der Kint S, Vissers L, van Schagen INLG, de Bruin J, van Gent P, et al. Interactions between cyclists and automated vehicles: Results of a photo experiment*. J Transp Saf Secur [Internet]. 2020;12(1):94–115. Available from: https://doi.org/10.1080/19439962.2019.1591556
14. Habibovic A, Lundgren VM, Andersson J, Klingegård M, Lagström T, Sirkka A, et al. Communicating intent of automated vehicles to pedestrians. Front Psychol. 2018;9(AUG).
15. Lee YM, Uttley J, Solernou A, Giles O, Romano R, Markkula G, et al. Investigating Pedestrians' Crossing

Behaviour During Car Deceleration Using Wireless Head Mounted Display: An Application Towards the Evaluation of eHMI of Automated Vehicles. 2020;252–8.

16. Hashimoto Y, Yanlei G, Hsu LT, Shunsuke K. A Probabilistic Model for the Estimation of Pedestrian Crossing Behavior at Signalized Intersections. In: IEEE Conference on Intelligent Transportation Systems, Proceedings, ITSC. 2015. p. 1520–6.
17. Tabone W, de Winter J, Ackermann C, Bärgman J, Baumann M, Deb S, et al. Vulnerable road users and the coming wave of automated vehicles: Expert perspectives. Transp Res Interdiscip Perspect [Internet]. 2021;9(December 2020):100293. Available from: https://doi.org/10.1016/j.trip.2020.100293
18. Li S, Sayed T, Zaki M, Mori G, Stefanus F, Khanloo B, et al. Automated Collection of Pedestrian Data through Computer Vision Techniques: https://doi.org/103141/2299-13 [Internet]. 2012 Jan 1 [cited 2022 Mar 19];(2299):121–7. Available from: https://journals.sagepub.com/doi/10.3141/2299-13
19. Helbing D, Molnár P. Social force model for pedestrian dynamics. Phys Rev E. 1995;51(5):4282–6.
20. Anvari B, Bell MGH, Sivakumar A, Ochieng WY. Modelling shared space users via rule-based social force model. Transp Res Part C Emerg Technol [Internet]. 2015;51:83–103. Available from: http://dx.doi.org/10.1016/j.trc.2014.10.012
21. Oxley JA, Ihsen E, Fildes BN, Charlton JL, Day RH. Crossing roads safely: An experimental study of age differences in gap selection by pedestrians. Accid Anal Prev. 2005;37(5):962–71.
22. Yannis G, Papadimitriou E, Theofilatos A. Pedestrian gap acceptance for mid-block street crossing. Transp Plan Technol. 2013;36(5):450–62.
23. Das S, Manski CF, Manuszak MD. Walk or wait? An empirical analysis of street crossing decisions. J Appl Econom. 2005;20(4):529–48.
24. Yang D, Li L, Redmill K, Ozguner U. Top-view trajectories: A pedestrian dataset of vehicle-crowd interaction from controlled experiments and crowded campus. IEEE Intell Veh Symp Proc. 2019;2019-June(Iv):899–904.
25. Knoblauch RL, Pietrucha MT, Nitzburg M. Field studies of pedestrian walking speed and start-up time. Transp Res Rec. 1996;(1538):27–38.
26. Chandra S, Bharti AK. Speed Distribution Curves for Pedestrians During Walking and Crossing. Procedia - Soc Behav Sci [Internet]. 2013;104:660–7. Available from: http://dx.doi.org/10.1016/j.sbspro.2013.11.160
27. Jeong E, Oh C, Lee S. Is vehicle automation enough to prevent crashes? Role of traffic operations in automated driving environments for traffic safety. Accid Anal Prev [Internet]. 2017;104(February):115–24. Available from: http://dx.doi.org/10.1016/j.aap.2017.05.002
28. Joshua Cregger, Margo Dawes, Stephanie Fischer, Caroline Lowenthal, Elizabeth Machek and DP. Low-Speed Automated Shuttles: State of the Practice Final Report [Internet]. 2018. Available from: https://rosap.ntl.bts.gov/view/dot/37060
29. Han Y, Yang J, Mizuno K, Matsui Y. Effects of Vehicle Impact Velocity, Vehicle Front-End Shapes on Pedestrian Injury Risk. Traffic Inj Prev. 2012;13(5):507–18.
30. Crandall JR, Lessley DJ, Kerrigan JR, Ivarsson BJ. Thoracic deformation response of pedestrians resulting from vehicle impact. Int J Crashworthiness. 2006;11(6):529–39.

31. Yang JK, Lövsund P, Cavallero C, Bonnoit J. A Human-Body 3D Mathematical Model for Simulation of Car-Pedestrian Impacts. J Crash Prev Inj Control. 2000;2(2):131–49.
32. Anderson RWG, Long AD, Serre T. Phenomenological continuous contact-impact modelling for multibody simulations of pedestrian-vehicle contact interactions based on experimental data. Nonlinear Dyn. 2009;58(1–2):199–208.
33. Peng Y, Chen Y, Yang J, Otte D, Willinger R. A study of pedestrian and bicyclist exposure to head injury in passenger car collisions based on accident data and simulations. Saf Sci [Internet]. 2012;50(9):1749–59. Available from: http://dx.doi.org/10.1016/j.ssci.2012.03.005
34. Hybrid III 50th Percentile Male Standing | Livermore Software Technology Corp. [Internet]. [cited 2022 Jan 18]. Available from: https://www.lstc.com/products/models/dummies/H3_50th_Standing
35. Self-Driving OLLI minibus - Global Motor Media [Internet]. [cited 2022 Jan 14]. Available from: https://www.globalmotormedia.com/self-driving-olli-minibus/?fbclid=IwAR39a9kw_o_sJx_okDNXVDJhLkuT7_g9-UYX61goD313m2_q2qRLSeElM9o
36. Crash Simulation Vehicle Models | NHTSA [Internet]. [cited 2022 May 12]. Available from: https://www.nhtsa.gov/crash-simulation-vehicle-models
37. Eppinger R, Sun E, Bandak F, Haffner M, Khaewpong N, Maltese M, et al. Automotive Restraint Evalation. Nthsa. 1999.
38. Schneck DJ, Bronzino JD. Biomechanics principles & Applications. 2002. 309 p.
39. Carollo F, Virzì Mariotti G, Naso V, Golfo S. Head, chest and femur injury in teenage pedestrian–SUV crash; mass influence on the speeds. Proc Inst Mech Eng Part D J Automob Eng. 2019;233(4):790–809.
40. Mariotti GV, Golfo S. Determination and analysis of the head and chest parameters by simulation of a vehicle-teenager impact. Proc Inst Mech Eng Part D J Automob Eng. 2014;228(1):3–20.
41. Mariotti GV. Head Injury Criterion: Mini Review. Am J Biomed Sci Res. 2019;5(5):406–7.
42. Bellavia G, Mariotti GV, Meccanica D, Palermo U. Development of an anthropomorphic model for vehicle-pedestrian crash test. 2007;62.
43. Namjoshi DR, Good C, Cheng WH, Panenka W, Richards D, Cripton PA, et al. Towards clinical management of traumatic brain injury: A review of models and mechanisms from a biomechanical perspective. DMM Dis Model Mech. 2013;6(6):1325–38.
44. Kong C, Yang J. Logistic regression analysis of pedestrian casualty risk in passenger vehicle collisions in China. Accid Anal Prev [Internet]. 2010;42(4):987–93. Available from: http://dx.doi.org/10.1016/j.aap.2009.11.006
45. Mizuno K. Head Injuries in Vehicle-Pedestrian Imp. 2000;109(May 2022):232–43.
46. Han Y, Yang J, Nishimoto K, Mizuno K, Matsui Y, Nakane D, et al. Finite element analysis of kinematic behaviour and injuries to pedestrians in vehicle collisions. Int J Crashworthiness. 2012;17(2):141–52.
47. Practice AB, Domain OD, Framework C. Automated Vehicle Safety Consortium ™ Best Practice Table of Contents. 2020.
48. Allen, James P., Natalie R. Myers, Thomas A. Carlson, James T. Stinson, Richard J. Liesen, Lance L. Larkin,

Ben Eubanks and JLD-P. Autonomous Vehicle Pilot at Joint Base Myer-Henderson Hall - Project Report Summary and Recommendations. 2020.

49. LEVESON NG, THOMAS JP. STPA Handbook. 2018.
50. Khastgir S, Birrell S, Dhadyalla G, Jennings P. The Science of Testing: An Automotive Perspective. SAE Tech Pap. 2018;2018-April:1–8.
51. De Miguel MÁ, Fuchshuber D, Hussein A, Olaverri-Monreal C. Perceived pedestrian safety: Public interaction with driverless vehicles. IEEE Intell Veh Symp Proc. 2019;2019-June(Iv):90–5.
52. Becker C, Brewer J, Yount L. Safety of the Intended Functionality of Lane- Centering and Lane- Changing Maneuvers of a Generic Level 3 Highway Chauffeur System. 2020;(DOT HS 812 879):145.
53. Mark_Groce__MTA_New_York_City_Transit_QueensBus.602b1e5a76057.png (799×450) [Internet]. [cited 2022 Mar 21]. Available from: https://img.masstransitmag.com/files/base/cygnus/mass/image/2021/02/16x9/Mark_Groce__MTA_New_York_City_Transit_QueensBus.602b1e5a76057.png?auto=format&fit=max&w=1200
54. Nie B, Li Q, Gan S, Xing B, Huang Y, Li SE. Safety envelope of pedestrians upon motor vehicle conflicts identified via active avoidance behaviour. Sci Rep [Internet]. 2021;11(1):1–10. Available from: https://doi.org/10.1038/s41598-021-82331-z
55. Nasernejad P, Sayed T, Alsaleh R. Modeling pedestrian behavior in pedestrian-vehicle near misses: A continuous Gaussian Process Inverse Reinforcement Learning (GP-IRL) approach. Accid Anal Prev [Internet]. 2021;161(July):106355. Available from: https://doi.org/10.1016/j.aap.2021.106355

8 APPENDIX: RESEARCH RESULTS

Sidebar Info

Program Steering Committee: NCHRP IDEA Program Committee
Month and Year: July 2022
Title: Safety Assessment of the Interaction between the Autonomous Shuttle Bus and Vulnerable Road Users

Project Number: Transit-98
Start Date: October 27, 2020
Completion Date: July 5, 2022

Project Category: IDEA Transit

Principal Investigator:
Sungmoon Jung, Professor
sjung@eng.famu.fsu.edu
850-410-6386

Title:

Safety of Autonomous Bus and Road Users

Subhead:

This project assessed the safety of autonomous buses against vulnerable road users. High-risk situations were analyzed to provide safety recommendations.

What Was the Need?

As more automated shuttle buses are deployed by different entities, new safety requirements emerge. New unsafe situations caused by vehicle or vulnerable road users include cybersecurity breach, sensor malfunction, and risk-taking behavior of road users. Thus far, studies on the automated vehicles and road users focused on detecting pedestrian, communication methods, and prediction of pedestrian's behavior. The main limitation of these studies was not considering the interaction between the autonomous vehicle and the road user. The innovation and unique aspect of this research was to model the interaction between the vehicle and the road user.

What Was Our goal?

The goal of the project was to assess the safety of autonomous shuttle buses against vulnerable road users. High-risk situations were analyzed to provide recommendations to improve safety.

What Did We Do?

In collaboration with our industry partner JTA, a closed tract testing was conducted using an autonomous shuttle bus. Field data on shuttle bus were also analyzed. However, the main part of the research was the development of the computer model to simulate the interaction between the autonomous shuttle bus and the road user. The computer simulation enabled exploration of safety-critical cases. The computer simulation consisted of modeling the overall

motion and basic decision-making process of the vehicle and pedestrian. Minimum gaps that pedestrians accept during road crossing were obtained from the Matlab simulation model. A finite element simulation model was developed to determine risk injury criteria for both head and chest if an unavoidable crash was to occur. Using the simulation and field crash data we were able to identify scenarios that can lead to hazardous situations regarding the pedestrians.

What Was the Outcome?

The outcomes of this research are as follows. 1) An autonomous shuttle bus was tested within a closed track by our industry partner JTA. 2) The vehicle and pedestrian models were developed to represent the motion of the vehicle and crossing pedestrian. 3) Using these models, a systematic pedestrian safety analysis was conducted to identify risk scenarios. Field crash data was also analyzed. The crossing, the bus station, and the roundabout were the most challenging type of interactions that autonomous vehicles can have regarding pedestrian interaction.

What Was the Benefit?

This report provides safety-critical cases and information to improve the safety for the autonomous shuttle bus. Any entity planning to deploy autonomous shuttle bus may find the research outcome helpful in their planning.

Images: 1) Stationary pedestrian test conducted by JTA at the Test &Learn Facility, 2) Schematic illustration of the interaction between the autonomous bus and vulnerable road users (VRU's)